DESIGN OF SUBSYSTEMS FOR A REPRESENTATIVE MODERN LEO SATELLITE

By

MARK WERREMEYER

A THESIS PRESENTED TO THE GRADUATE SCHOOL
OF THE UNIVERSITY OF FLORIDA IN PARTIAL FULFILLMENT
OF THE REQUIREMENTS FOR THE DEGREE OF
MASTER OF SCIENCE

UNIVERSITY OF FLORIDA

2013

To my family, friends, and colleagues for all their support

ACKNOWLEDGMENTS

I would like to thank my family, Kathleen, Mark, and Melissa Werremeyer for their life-long support. Without their unconditional love and the countless hours they have spent at my side, I would have never reached this point.

I would also like to show my deep appreciation to my advisor and chair, Dr. Norman Fitz-Coy. Without his knowledge and support, I would never have had the opportunity to work on the wonderful project that is DebriSat. His dedicated pursuit of space technology has provided opportunities for many graduate and undergraduate students at the University of Florida to participate in space research for which myself and many others are extremely thankful. In addition, I would like to acknowledge Dr. John Conklin for his support as a member on my committee.

I would also like to thank my friends in Tampa, Gainesville, and now other parts of the United States. Sheldon Clark has worked at my side since we were twelve years old in Boy Scouts, through high school, our aerospace engineering degrees, and now DebriSat. He will always be the best teammate I could have. Thank you to Hillary Silvestri for more than four years of constant love, support, and delicious meals. The adult leaders from Troop 686: Charles Anderson, Blair Lindsay and many others who have selflessly dedicated their lives to mentoring our younger generations, including myself – I will always love and respect you. Thank you to Jose Godinez-Samperio who remains an inspiration to me with the obstacles that he has overcome - I am grateful that I can call you my friend. Thank you to the Russells, who have been close family friends for more than twenty years and to Scott, whom was taken from us at an early age but will always have a place in all of our hearts.

Lastly, I would like to thank our liaisons from the NASA Orbital Debris Programs Office, USAF Space and Missile Systems Center, The Aerospace Corporation, and Jacobs Engineering for their support of DebriSat. Without you, this project would not have been possible and our interactions have given me many invaluable insights and experiences.

TABLE OF CONTENTS

LIST OF TABLES

LIST OF FIGURES

LIST OF ABBREVIATIONS

2D	Two-dimensional
ADCS	Attitude determination and control system
AEDC	Arnold Engineering Development Center
AN	Army-Navy
C&DH	Command and data handling
CAD	Computer aided design
CIC	Coverglass interconnect cell
COGEX	Cool gas experiment
COPV	Composite-overwrapped pressure vessel
COTS	Commercial off-the-shelf
CPL	Capillary-pumped loop
DC	Direct current
EDU	Engineering development unit
EPS	Electrical Power System
FDV	Fill and drain valve
FEA	Finite element analysis
IMU	Inertial measurement unit
LEO	Low Earth orbit
LI-ION	Lithium ion
MLI	Multi-layer insulation
MS	Margin of safety
NASA	National Aeronautics and Space Administration
NMU	Nitrous management unit
NPT	National pipe thread

OD	Outer diameter
RoHS	Restriction of Hazardous Substances
SME	Subject-matter expert
SOCIT	Satellite Orbital debris Characterization Impact Test
TT&C	Telemetry tracking and command
UCS	Union of Concerned Scientists
UHF	Ultra-high frequency
USAF	United States Air Force
VHF	Very high frequency

Abstract of Thesis Presented to the Graduate School
of the University of Florida in Partial Fulfillment of the
Requirements for the Degree of Master of Science

DESIGN OF SUBSYSTEMS FOR A REPRESENTATIVE MODERN LEO SATELLITE

By

Mark Werremeyer

August 2013

Chair: Norman Fitz-Coy
Major: Aerospace Engineering

This thesis discusses the design of subsystems for a representative modern low Earth Orbit (LEO) satellite. Specifically, the subsystems presented were designed for inclusion on DebriSat, a 50 kg satellite intended to be representative of modern LEO satellites ranging from 1-5000 kg terms of its components, materials used, and fabrication procedures. A LEO satellite survey was conducted that utilized the Union of Concerned Scientists (UCS) satellite database, with selected satellites emphasizing those launched after 1990 and next-generation satellites expected to launch in the near future. Specifically, fifty U.S. and European satellites were studied in detail to determine appropriate subsystems and components for use in a representative modern LEO satellite. As a result of this study and further consultation with subject-matter experts, particular components and subsystems were down selected for inclusion in the DebriSat design (e.g. sun sensors and reaction wheels are implemented rather than horizon sensors and passive magnetics due to their prevalence on the satellites surveyed). After these components were determined, they were integrated into complete subsystem designs. Finally, this thesis details how these representative components and subsystems are to be fabricated. Due to the prohibitively high costs of flight hardware,

donated and rejected flight units are used in some instances, while non-functional emulations are used in others. DebriSat is a collaborative effort with NASA Orbital Debris Programs Office, the USAF Space and Missile Systems Center, and The Aerospace Corporation.

CHAPTER 1
INTRODUCTION

Background

Orbital debris is a growing concern to existing and future space assets. After the collision of Iridium-33 and Cosmos-2251 in 2009, the NASA standard breakup model under-predicted the resulting fragments of the Iridium satellite. Modern materials used in Iridium are suspected as the cause of the debris fragment under-prediction, particularly carbon fiber composites, multi-layer insulation (MLI), and coverglass interconnected cells (CICs). Therefore, improved fidelity is needed in existing satellite breakup models to obtain more reliable impact risk assessments. Current breakup models are based on the Satellite Orbital debris Characterization Impact Test (SOCIT) series tests conducted in 1992 that used a Navy TRANSIT satellite constructed in the 1960's. Modern satellites are much different from those constructed in the 1960's, hence, a modern satellite impact test using modern materials is needed. DebriSat is a 50 kg microsatellite that aims to represent a wide variety of low Earth orbit (LEO) satellites, particularly modern satellites launched since the 1990's and next generation satellites expected to launch in the near-future. While only 50 kg, the DebriSat design is intended to be representative of modern LEO satellites ranging from 1-5000 kg. DebriSat will be used in a hyper velocity impact test with the overall purpose to investigate the debris fragments generated after an on-orbit collision of modern LEO satellites, using modern materials and construction methods.

This thesis describes various subsystems deemed appropriate for a representative modern LEO satellite, in particular, structural, attitude determination and control, propulsion, and thermal management systems. These subsystems were

developed specifically for use on DebriSat and in its eventual hypervelocity impact which will be conducted at the Arnold Engineering Development Center (AEDC) in Tennessee.

Scope

The DebriSat project is a collaborative effort among multiple organizations, namely the NASA Orbital Debris Programs Office, USAF Space and Missile Systems Center, Jacobs Engineering, The Aerospace Corporation, and the University of Florida. As part of this collaboration, the University of Florida team was responsible for the design and fabrication of DebriSat. The UF team is led by Dr. Norman Fitz-Coy, director of Space Systems Group, and currently consists of Sheldon Clark, Fabian Marseille, and Mark Werremeyer. This thesis focuses on the subsystems developed by Mark Werremeyer, namely the structures, attitude determination and control system (ADCS), propulsion system, and thermal management system. It is noted, however, that a preliminary ADCS was developed by Ann Dietrich with the support of Kevin Lane in April 2012 [1]. The ADCS design presented in this thesis is an evolution of that preliminary design as Mark Werremeyer became responsible for its continued development in May 2012. Additional subsystems that would be expected on a LEO satellite such as the electrical power system, command and data handling, telemetry tracking and command, and payload were developed by Sheldon Clark and therefore are outside the scope of this thesis.

The designs presented are proposed as representative modern LEO satellite subsystems in terms of their materials, components, and construction methods. Initially, space-qualified commercial units were sought; however, these units were prohibitively expensive. Additionally, flight rejected and engineering development units (EDUs) were

sought at a reduced price, but many vendors were unable to provide these except for in a few instances. Therefore, many components presented are designed as non-functional emulated units since the effects of component functionality (e.g. spinning reaction wheels) are assumed negligible in terms of the overall impact behavior.

In the next chapter, a LEO satellite survey is discussed and how it was used to down select components for use in a representative modern LEO satellite.

CHAPTER 2
LEO SATELLITE SURVEY

A survey of current and recent low Earth orbit (LEO) unmanned missions was performed by the DebriSat team to determine typical components and characteristics of satellites that operate in LEO. This survey was then used to drive the selection and design of components for DebriSat. A comprehensive list of LEO missions was obtained from the Union of Concerned Scientists [2] and organized by dry mass to determine an identifiable distribution of LEO missions. This distribution was then scaled to a selection of 50 modern missions analyzed for physical characteristics including component selection, materials, and mission details such that the ratio of the number of satellites in any two mass ranges remains sufficiently constant. Figure 2-1 shows the distribution of the satellites used in the survey as it compares to the distribution in the UCS database.

The survey showed that there is strong correlation between the components that are used in LEO missions and the dry mass of the mission. Therefore, the design of DebriSat was driven primarily by the components deemed either standard among all mass ranges, significant to two or more mass ranges, a new design standard since 1992, or trending towards increased use in the future. However, the survey was found to be deficient in representation of extremely detailed designs and of non-U.S. or European backed missions (specifically Russia and China) due to the restrictions and limitations of information available in the public domain as shown in Figure 2-2. Therefore, the subsystems presented may be considered deficient in representing Russian and Chinese satellites. Emphasis was placed on recently launched satellites, i.e. missions in the 1997 to 2011 timeframe. Additional results from the survey and its analysis are outlined in Clark, et al. [3] as well as Clark, et al. [4].

Figure 2-3 and Figure 2-4 depict the percent usage of ADCS sensors and actuators with respect to each mass category. Sun sensors and magnetometers were prevalent in every mass category and are therefore included in DebriSat. While star trackers were not used on any satellites in the 10-100 kg category, they were heavily used in the 100-2000 kg mass ranges. Therefore, to create a representative LEO satellite, star trackers were considered a necessary component. A trend of increasing gyroscope use was also seen as the satellite mass increased. However, since this survey was created from public domain information, the terminology from one satellite to the other might have been inconsistent. In particular, the terms “gyroscope” and “inertial measurement unit (IMU)” might have been used interchangeably which would therefore show that these technologies are prevalent in almost every mass range. Due to the prevalence of both, an IMU was justified for inclusion in the design [4].

As seen in Figure 2-4, magnetorquers were prevalent in every mass range, while reaction wheels were employed in the 100-5000 kg mass ranges. Only smaller satellites used passive actuators, such as passive magnetic and reflection strips, therefore these were not chosen for inclusion in the design. In order to represent actuators typically used in a LEO satellite, reaction wheels and magnetorquers were incorporated into the ADCS design [4].

Figure 2-5 illustrates propulsion system usage based on mass as determined from the survey. As seen in the figure, propulsion systems are prevalent in all LEO satellites larger than 100 kg, and are heavily utilized in the 1000-2000 kg group. Note that propulsion systems are relatively rare for small satellites, including DebriSat’s own mass category, 10-100 kg. However, while uncommon for a satellite of DebriSat’s mass,

a propulsion system is necessary to accurately represent the broader range of LEO satellites and was therefore included in the design [4]. Additional inferences can be made as to the use of propulsion systems on LEO satellites when one considers that thrusters are rarely used for ADCS according to Figure 2-4. Therefore, it is likely that LEO propulsion systems are employed mostly for orbit maintenance.

A survey of representative telemetry tracking and command (TT&C) was performed based on the frequency band usage of LEO satellites as shown in Figure 2-6. The figure illustrates the usage of typical communication bands within each mass range. S band frequencies are the most common between all mass ranges, while UHF and VHF bands are prevalent to smaller mass missions. It is observed that the X band is commonly used throughout larger mass missions though to a lesser degree than the S band. Based on these results, a representative satellite would consider including TT&C components that operate in VHF, UHF, S, and/or X band frequencies [3]. It is also noted that LEO satellites are not typically limited to the usage of one communication band. Multiple bands are often used in TT&C systems while communication payloads would also utilize some of the bands shown. Therefore, it is conceivable that a representative satellite would include the UHF, VHF, S band, and X band all in one satellite.

A survey of common used batteries in LEO satellites is shown in Figure 2-7. Li-ion is most prevalent and has increased usage among smaller satellites, dominating the 1-10 kg range. Nickel-hydrogen and nickel-cadmium batteries have increasing usage in the larger mass ranges, with nickel-hydrogen dominating usage in the 2000-5000 kg range [3]. Li-ion, while already in use on a number of LEO satellites, is also expected to

become more common in future LEO satellites based on discussions with an SME in spacecraft electrical power systems (EPS)[1]. Since Li-ion is expected to be used more frequently in the future and because it is already common in modern LEO satellites, Li-ion batteries were selected for use in a representative EPS.

The payload survey classified each satellite by their primary mission: Earth observing, remote sensing, communication, and technology demonstration. The survey reveals that communication payloads and Earth observing are the most prevalent class of LEO payloads. Communication payloads were identified as common constellation payloads – particularly that one common design is included over several dozen satellites, such as Iridium. Earth observing missions typically use imagers that operate in either the near-infrared or visible wavelength spectrum. In addition, the number of payload instruments per mission was typically greater than one. Thus, multiple payload instruments should be considered for a representative design. The complexity and uniqueness of one mission payload compared to another also led to the conclusion that a truly representative payload contained in a single satellite is very difficult to identify. Due to the prevalence of Earth observing and remote sensing payloads, an optical imager and near-infrared spectrometer were selected as representative payloads. However, to also recognize the prevalence of communications payloads in LEO satellites and due to the prevalence of these particular bands in other TT&C subsystems, a combination of X band, S band, UHF, and VHF antennas were selected for inclusion in the representative TT&C subsystem.

[1] Joseph Nemanick (Spacecraft Electrical Power Systems Expert, The Aerospace Corporation), in discussion with Sheldon Clark, January 30, 2013.

To summarize, the results of the LEO satellite survey justify the inclusion of a number of components and subsystems into the DebriSat design. In particular, components and subsystems used in larger LEO satellites (100-5000 kg) are justified for inclusion on a 50 kg satellite that is “representative” of the broader range of LEO satellites. The inclusion of the propulsion system is a significant consequence, since propulsion systems would be rare for a 50 kg satellite under normal circumstances. Additionally, the justification for multiple communication bands is made due to their prevalence in TT&C systems as well as their prevalence of use in LEO payloads.

In the next chapter, the overall design of DebriSat is presented with a breakdown of subsystems and their respective components as selected based upon the results of the LEO satellite survey.

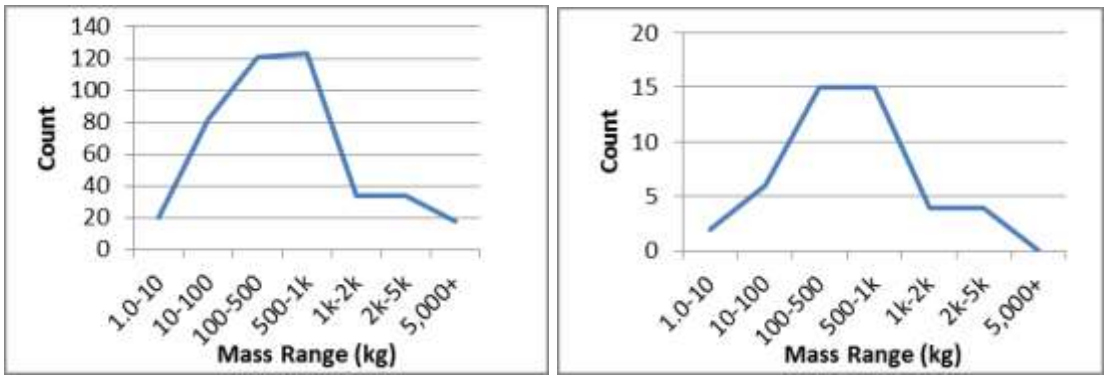

Figure 2-1. Satellite mass distribution. A) distribution of 467 satellites from UCS database, B) distribution of 50 satellites surveyed. Adapted from Clark, S., Lane, K., Strickland, T., Fitz-Coy, N., and Liou, J.-C., "Defining a Typical Low Earth Orbit Satellite – Using Historical Mission Data to Aid Orbital Debris Mitigation," (Page 2, Figures 1 and 2) in AIAA Region 2 Student Conference, Orlando, 2012.

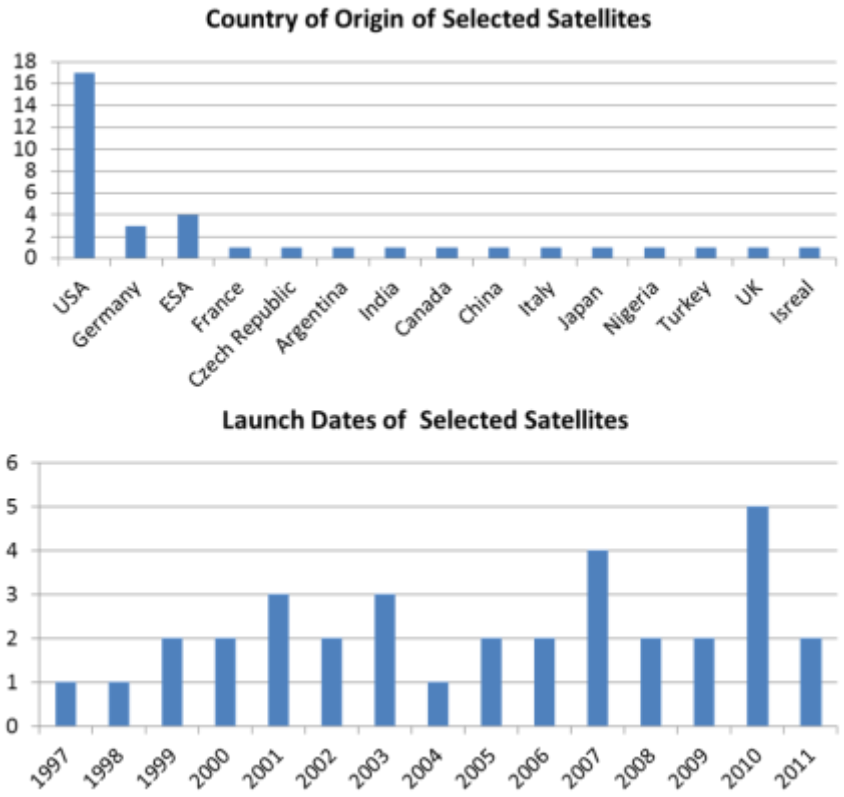

Figure 2-2. Launch dates and origins of selected satellites

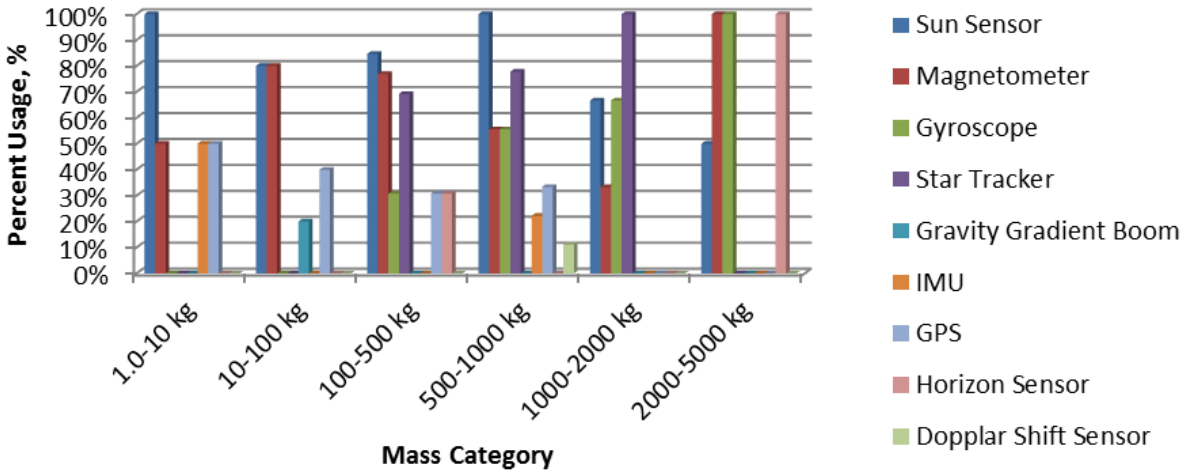

Figure 2-3. ADCS sensor usage by mass. Adapted from Clark, S., Dietrich, A., Werremeyer, M., Fitz-Coy, N., and Liou, J.-C., "Analysis of Representative Low Earth Orbit Satellite Data to Improve Existing Debris Models," (Page 3, Figure 1) in *AIAA Region 2 Student Conference*, Orlando, 2012.

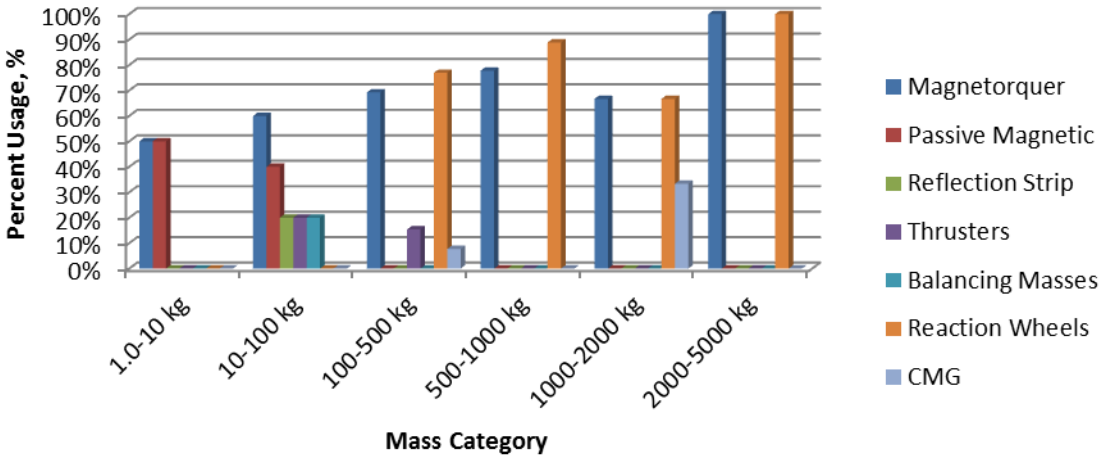

Figure 2-4. ACDS actuator usage by mass. Adapted from Clark, S., Dietrich, A., Werremeyer, M., Fitz-Coy, N., and Liou, J.-C., "Analysis of Representative Low Earth Orbit Satellite Data to Improve Existing Debris Models," (Page 3, Figure 2) in *AIAA Region 2 Student Conference*, Orlando, 2012.

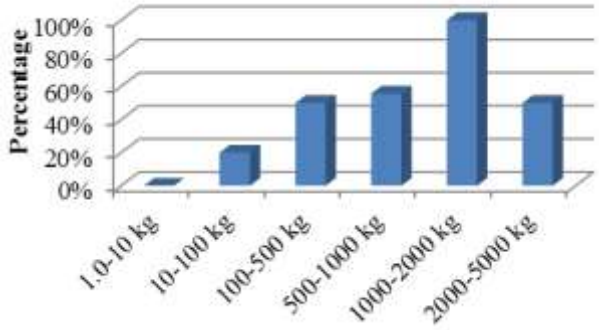

Figure 2-5. Propulsion system usage by mass. Adapted from Clark, S., Dietrich, A., Werremeyer, M., Fitz-Coy, N., and Liou, J.-C., "Analysis of Representative Low Earth Orbit Satellite Data to Improve Existing Debris Models," (Page 5, Figure 4) in *AIAA Region 2 Student Conference*, Orlando, 2012.

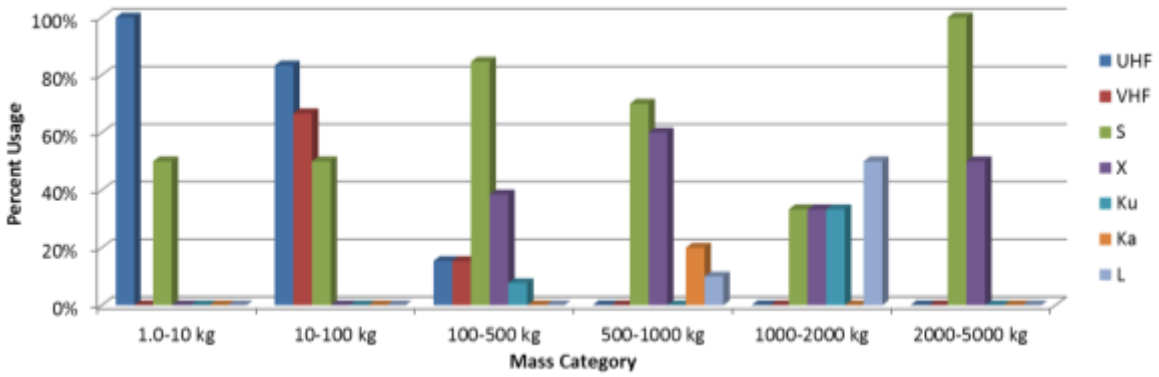

Figure 2-6. LEO communication bands by mass. Adapted from Clark, S., Lane, K., Strickland, T., Fitz-Coy, N., and Liou, J.-C., "Defining a Typical Low Earth Orbit Satellite – Using Historical Mission Data to Aid Orbital Debris Mitigation," (Page 4, Figure 4) in *AIAA Region 2 Student Conference*, Orlando, 2012.

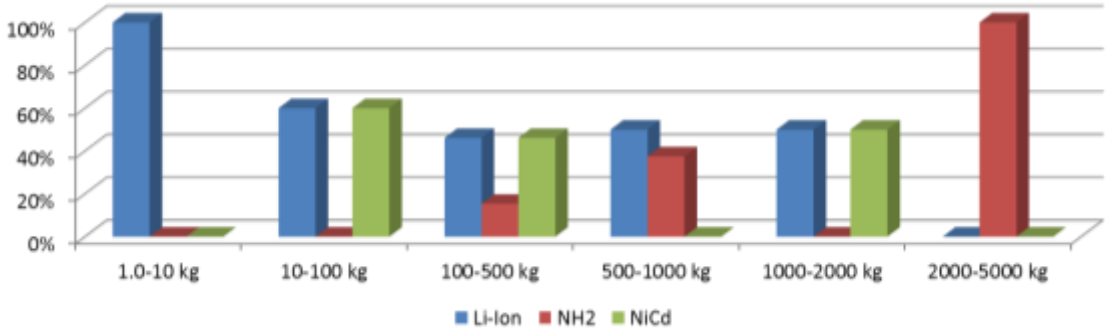

Figure 2-7. LEO batteries by mass range. Adapted from Clark, S., Lane, K., Strickland, T., Fitz-Coy, N., and Liou, J.-C., "Defining a Typical Low Earth Orbit Satellite – Using Historical Mission Data to Aid Orbital Debris Mitigation," (Page 3, Figure 3) in *AIAA Region 2 Student Conference*, Orlando, 2012.

CHAPTER 3
SYSTEMS OVERVIEW

The DebriSat design is intended to represent the overall system makeup and physical characteristics of unmanned LEO missions ranging from 1-5000 kg in mass. The overall system contains a wide variety of components that are not typically found on a satellite of DebriSat's size but are found on satellites in other mass ranges. Thus the design is not intended to be functional but rather seeks to be representative of component material and functionalities as much as possible across a broad range of satellite platforms. The complete DebriSat is shown in Figure 3-1.

System Level Design

The DebriSat design is a non-functioning satellite that emulates the materials and functionalities of modern LEO space missions. Basic system characteristics are given in Table 3-1.

As shown in Figure 3-2, the satellite is a hexagonal body containing six compartmentalized bays and a seventh cylindrical bay about the central axis. Two hexagonal panels serve as the nadir and zenith facing structural elements. Components are mounted to side, rib, and hexagonal panels of the DebriSat structure. Figure 3-2 shows an orthogonal view of the nadir-facing hexagonal panel and various bays.

Each satellite side panel and rib is constructed of two carbon fiber face sheets and a sandwiched aluminum honeycomb core. Individual components are mounted to these panels primarily through fastened inserts into the honeycomb core. Viewing from the zenith panel to the nadir hexagonal panel, the bay count begins with the first Li-ion battery box and proceeds clockwise through bay 2 with the optical imager to bay 6 containing the power conditioning and distribution unit and a spectrometer. A detailed

overview of this layout is given in Figure 3-3. In addition to the components mounted to the side paneling, several components are located and fastened within the central volume of the structure. These components are considered part of bay 7. This bay contains the propulsion system and various other components mounted to the hexagonal panels and structural ribs. Mounting to the structure is done on the hexagonal base panels or the structural ribs. Also included is the electrical distribution cabling and plumbing for the satellite's propulsion system. Figure 3-4 identifies the propulsion system, heat pipes, and solar panels from the zenith perspective.

Mass Budget

Emphasis was on the DebriSat subsystem masses to ensure each subsystem mass fraction was in-line with historical values. Table 3-2 shows the DebriSat subsystem mass budgets and the predicted design mass for a 50 kg target mass.

The predicted design mass was primarily calculated using a combination of computer generated solid modeling and subsystem design assumptions. Each modeled component was assigned either a defined mass or a material property based on availability of precise mass properties. The majority of emulated components which will require machining are estimated using assigned material properties, whereas several components were assigned a set mass based on in-house measurements or details from commercial vendors. Combining these approaches yielded a predicted system mass of 49.77 kg. A contingency was added to the mass based on several assumptions:

- Some fasteners were not included in the solid model design and therefore were not included in the overall structure mass
- A complete wiring scheme is not included in the models; therefore an estimation of wire mass is included

- Additional integration components such as epoxies and thermal compounds are not included
- Variations in material properties and irregularities in the solid models

In the next chapter, the DebriSat structure is discussed in detail, including its design, fabrication, and assembly.

Table 3-1. Top-level DebriSat characteristics

Project Title:	DebriSat
Target Mass:	50 kg
Physical Envelope (including extended components):	84 cm (lg.) x 61 cm (wd.) x 68 cm (ht.)
Stabilization:	3-axis
Deployables:	Yes (partially-deployed)

Table 3-2. DebriSat mass budget

Subsystem	Predicted Design Mass (kg)	Contingency (kg)
ADCS	4.46	0.44
C&DH	1.90	0.11
EPS	12.96	1.23
Payload	11.67	1.15
Propulsion	4.10	0.42
Structure	10.73	1.07
Thermal	1.00	0.14
TT&C	2.77	0.28
TOTAL	49.59	4.84

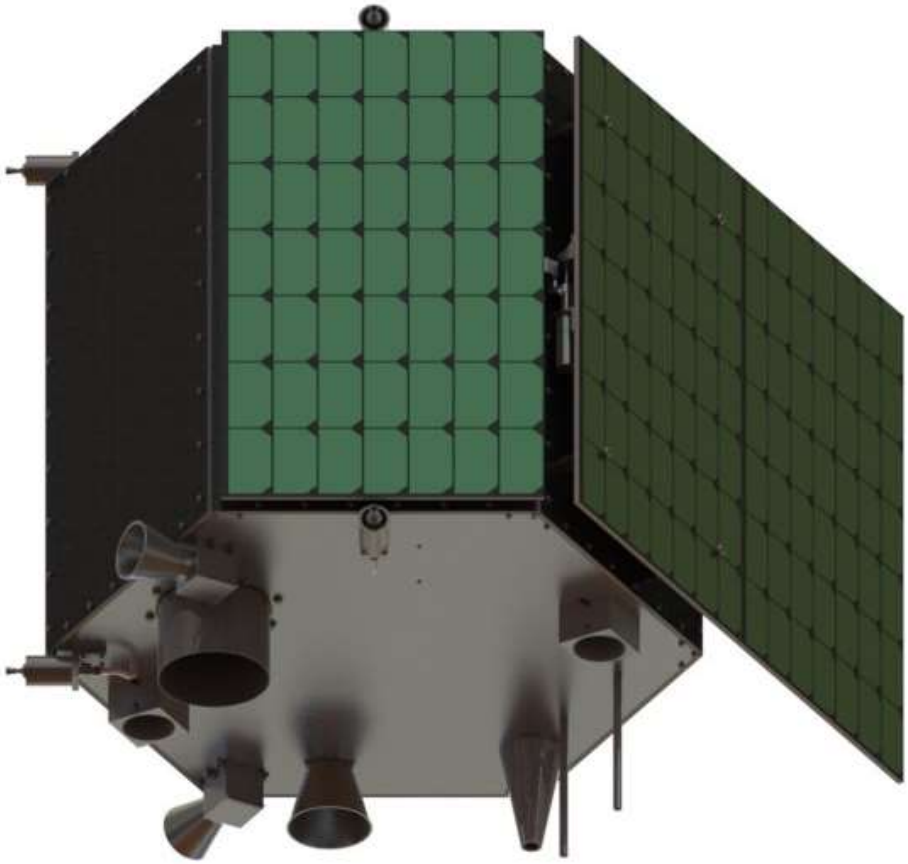

Figure 3-1. External view of DebriSat

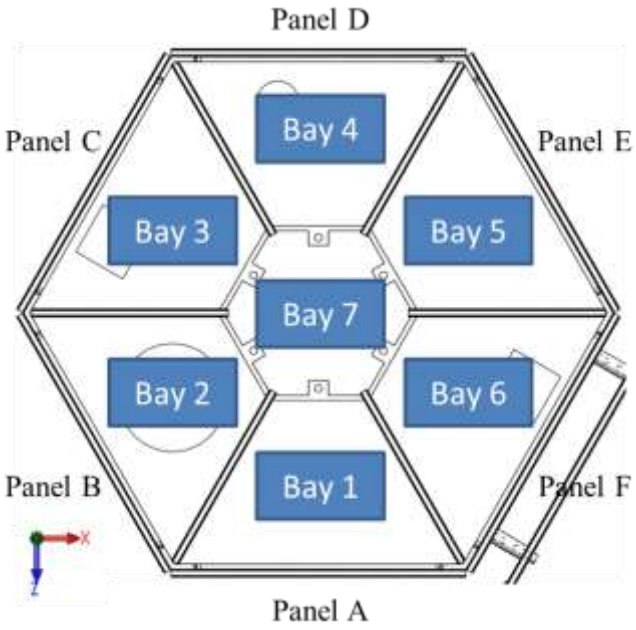

Figure 3-2. Bay assignments

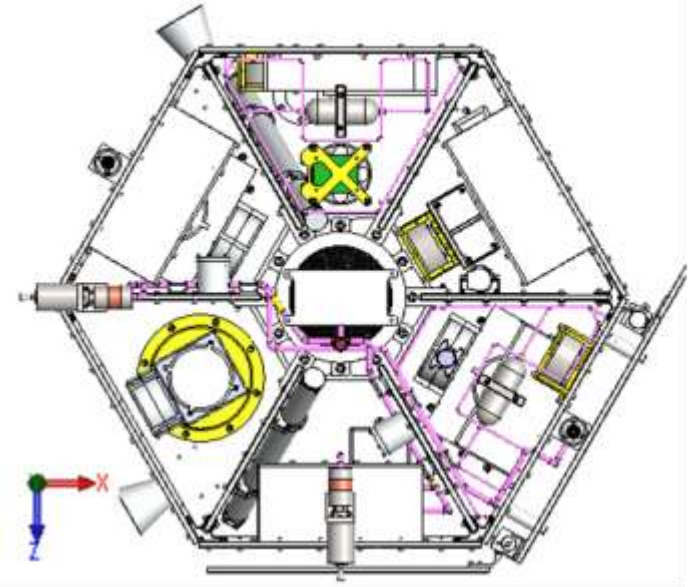

Component Identification	
1 – Flight Computer	13 – Telemetry Avionics (2)
2 – Data Recorder	14 – Fill Drain Valve
3 – Reaction Wheel (4)	15 – Star Tracker (2)
4 – X-Band Conical Feed Horn Antenna	16 – Sun Sensor (4)
5 – Optical Imager	17 – Payload Support Module
6 – Solenoids (3)	18 – Magnetometer
7 – Power Conditioning and Distribution	19 – ADCS Avionics
8 – Spectrometer (2)	20 – S-Band Helical Antenna
9 – Thermal Reservoir	21 – Propulsion Avionics
10 – Omni-Directional Antenna (2)	22 – Magnetorquer (3)
11 – COPV	23 – Inertial Measurement Unit
12 – Li-ion battery box (3)	24 – Thrusters (6)

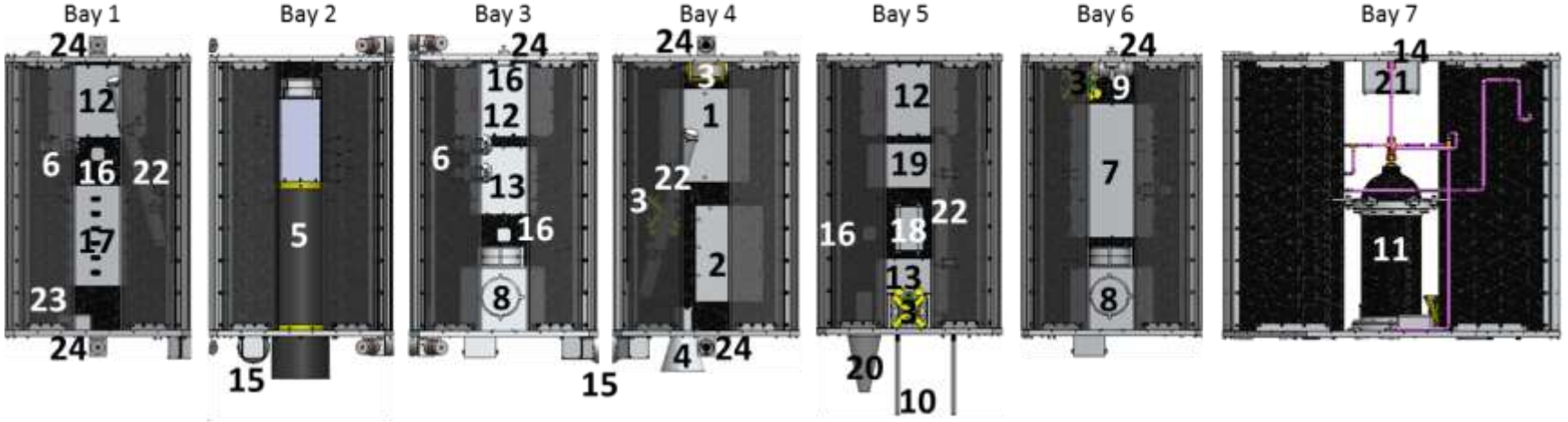

Figure 3-3. Component layout

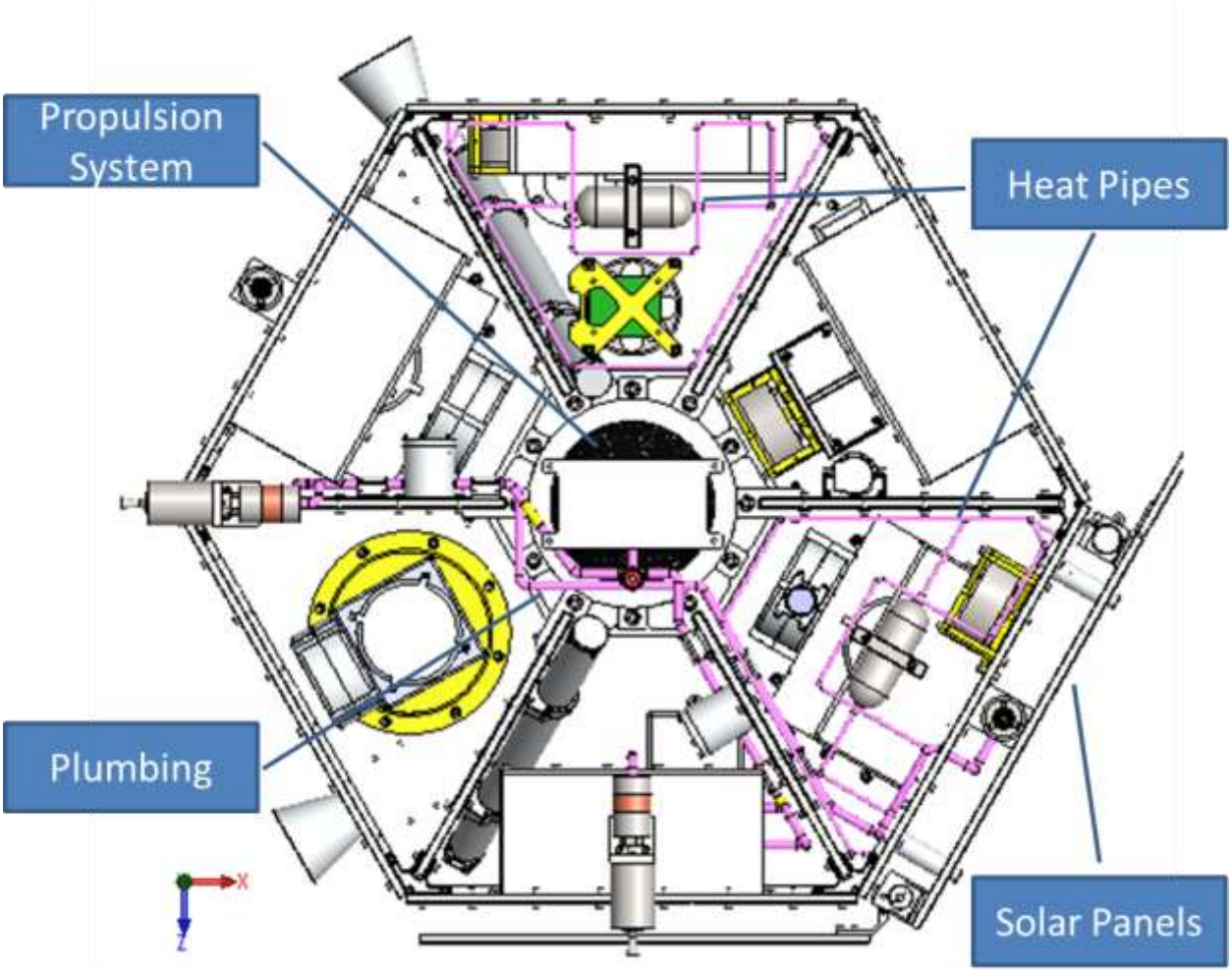

Figure 3-4. Internal view from nadir panel

CHAPTER 4
STRUCTURES

Assumptions

The following assumptions were used in the structure design:

- Aluminum is typical for longerons and panels
- Carbon fiber composite panels with aluminum honeycomb cores are typical
- The structure should withstand typical launch loads

It is realized that titanium is used in some structural designs. However, titanium is not included because it is believed that the material's use is declining among modern satellite missions. Also, a mixture of carbon fiber composite and aluminum panels are used to represent both materials. Composite panels are used for six sides, while aluminum is used for the nadir and zenith panels.

Design

The DebriSat structure is a hexagonal prism that is 500 mm tall with sides that are 300 mm wide each. Longerons are placed at all six corners of the hexagon and composite ribs were added to withstand launch loads. The composite ribs extend from each corner of the hexagon towards the center. Six composite side panels are attached on the outside of the longerons and edges of the hexagonal panels. The composite side panel and composite rib designs have an aluminum honeycomb core with carbon fiber cover sheets. Three composites panels are also used in a deployable array that is mounted to Panel F. A CAD model of the structural design with some composite side panels removed is shown in Figure 4-1.

The deployable panel structure is shown in Figure 4-2. Four aluminum 6061 standoffs connect the deployable panel structure to Panel F, with clearance for a deployable mechanism to fit between. Four spring hinges are used to connect an

additional two solar panels. The solar panels are the same material and dimension as the composite side panels, with M55J face sheets and an aluminum honeycomb core. The solar panels will be in a partially-deployed configuration during impact. The deployable array is shown in the partially-deployed configuration in Figure 4-2.

Component Selection

Table 4-1 lists the components of the structural system. All structural components require custom fabrication. The composite panel designs can be purchased from a composite panel manufacturer capable of accommodating custom composite panel designs. The composite panel manufacturer will provide the aluminum honeycomb and carbon fiber face sheets as a complete assembly with potted-in inserts for fasteners and any heat pipes already integrated. Initially M55J face sheets were selected but the cost would be prohibitively expensive due to DebriSat's small M55J requirement. Therefore, a fiber with similar material properties that is commercially available, M46J, was selected as a viable alternative. Both M55J and M46J are space-qualified fibers. Hexagon panels and all longerons are to be anodized to MIL-A-8625, Type III, Class 1, 0.0508 mm (2.0 mil) coating thickness.

Composite Panels

Figure 4-3 shows the composite panel sandwich design for panel A (with an access hole for a DebriSat sun sensor). A similar panel is used for the other composite side panels, composite ribs, and solar panels. The honeycomb core material is 5 mm thick Hexweb CR-PAA 3/16-5052-.001, which designates the material, cell size (in), alloy, and foil thickness (in) in that order. The CR-PAA indicates anodized and the honeycomb has a cell size of 4.8 mm (3/16 in), is made of aluminum 5052, and has a foil thickness of 0.025 mm (0.001 in). The two face sheets are made of Torayca M46J

carbon fiber in a quasi-isotropic laminate with eight plies normalized to 60% fiber volume and an approximate ply thickness of 0.61 mm (0.0024 in). The selected ply orientations are 0/45/-45/90/90/-45/45/0. Each composite side panel assembly is 300 mm wide by 500 mm tall, with an assembled thickness of approximately 6 mm. Each composite rib is 200 mm wide, 490 mm tall and 8.0 mm thick.

Revisions were necessary in the composite panel material selection due to difficulties encountered in identifying a supplier of M55J fiber. This difficulty was mostly due to the fact that M55J is not typically kept in stock but rather is only manufactured in dedicated productions runs for a specific program requirement. Since the DebriSat project requires a relatively small quantity of M55J, suppliers were unable to provide this fiber. The M46J fiber was identified as a readily available candidate replacement. M46J is a slightly lower modulus (fiber modulus of 426 GPa versus 540 GPa for M55J), and slightly higher strength (fiber strength of 4,210 MPa versus 4,020 MPa for M55J) fiber system [5] and [6]. According to a spacecraft structures SME, it was estimated that there would be about an 11% lower natural frequency and roughly 4% higher strengths and pointed out that while M46J has been qualified for use in space, M55J is much more prevalent[2]. Additionally, M46J was compared with M55J using finite element analysis (FEA) under launch loading conditions and these results are presented in Chapter 8. Material data sheets for M46J and M55J are provided in Appendix.

Longerons

The longeron design is shown in Figure 4-4. The longeron connects the nadir and zenith hexagonal panels and provides a flat surface for mounting the composite

[2] Scott Peck (Spacecraft Structures Expert, The Aerospace Corporation), in discussion with author, January 4, 2013.

side panels. There are six longerons in the DebriSat design, one at each corner of the hexagonal panels. The longeron is 480 mm long, 5 mm thick, and uses four M4 fasteners to connect to the nadir and zenith hexagonal panels. There are nine M3 clearance holes to facilitate bolts along the structural rib's outer vertical edge. Connecting the longeron to the composite ribs in this manner is intended to increase the structural rigidity of DebriSat.

Hexagonal Panels

The hexagonal panel design for the nadir facing panel is shown in Figure 4-5. The panel has sides of 300 mm length and is 10 mm thick. 7 mm of material is cut out of the panel to create the webbing structure shown, with each webbing feature being 5 mm wide. The central hexagon webbing has a circular bolt pattern for mounting the propulsion system and access holes to mount the optical payload, spectrometers, and communication antenna.

The hexagonal panel design for the zenith facing panel is shown in Figure 4-6. The panel also has sides of 300 mm length and is 5 mm thick. The zenith panel has a similar webbing structure to the nadir panel, being 10 mm wide and requiring a 7 mm depth cut out from the rest of the panel. The central hexagon webbing is 110 mm wide. This panel also serves as a radiator for the thermal management system.

Rib Mounting Brackets

Rib mounting brackets were added so that the structural composite ribs could be mounted to the zenith and nadir panels. Four brackets are used on each rib, two on the nadir side and two on the zenith side. The brackets are secured to the webbing of the nadir and zenith panels using eight M3 bolts.

Composite Ribs

The composite ribs are shown as they would be integrated with the longerons and rib mounting brackets in Figure 4-8. Six of these assemblies are positioned radially about DebriSat's longitudinal axis, providing structural integrity to compression, tension, and torsional loading of the DebriSat structure. The ribs are secured into the slotted longerons with nine bolts, while the rib mounting brackets use eight bolts at each end to secure the composite rib the webbing of the nadir and zenith hexagonal panels.

Deployment Mechanism

The deployment mechanism shown in Figure 4-9 provides a representative and stiff solar panel deployment. The mechanism utilizes an over-center latch design to achieve a stiff deployment state. Two deployment mechanisms are implemented in the design, one for each deployed panel. There is a 60 degree range of motion before the latch reaches the locked position, allowing the deployable panels to be positioned parallel to the sides of DebriSat or in a single plane as a deployed solar array. The mechanism shown in Figure 4-9 is shown in the undeployed and unlocked position at 60 degrees (60 degrees being the stowed position and 0 degrees being deployed).

Summary

Masses for the structural components are tabulated in Table 4-2. The DebriSat structure is predicted at 10.73 kg which is slightly below typical structural mass for a 50 kg satellite. A 10% contingency is added for each mass subtotal. This contingency accounts for mounting fasteners, variations in machining, and any other irregularities not accounted for in the CAD model. The materials used are aluminum 6061 for longerons and hexagonal panels, M46J for composite panel face sheets, and aluminum 5052 honeycomb for composite panel cores.

In the next chapter, the design, fabrication, and assembly of the DebriSat attitude determination and control system is discussed.

Table 4-1. Structure components

Component	Material	Supplier	Quantity
Hexagon Panel	Aluminum 6061	Manufactured	2
Longeron	Aluminum 6061	Manufactured	6
Composite Vertical Rib	Hexweb CR-PAA 3/16-5052-.001 Torayca M46J	Manufactured	6
Composite Panel	Hexweb CR-PAA 3/16-5052-.001 Torayca M46J	Manufactured	9
Solar Panel	Hexweb CR-PAA 3/16-5052-.001 Torayca M46J	Manufactured	3

Table 4-2. Structural component masses

Component	Mass (kg)	Quantity	Mass Subtotal (kg)	Contingency (kg)
Longeron	0.60	6	3.60	0.36
Composite Rib	0.18	6	1.08	0.11
Zenith Panel	1.70	1	1.70	0.17
Nadir Panel	1.60	1	1.60	0.16
Composite Side Panel	0.27	6	1.62	0.16
Solar Panel	0.27	3	0.81	0.08
Rib Bracket	0.01	12	0.12	0.01
Deployment Mechanism	0.10	2	0.20	0.02
		TOTAL	10.73	1.07

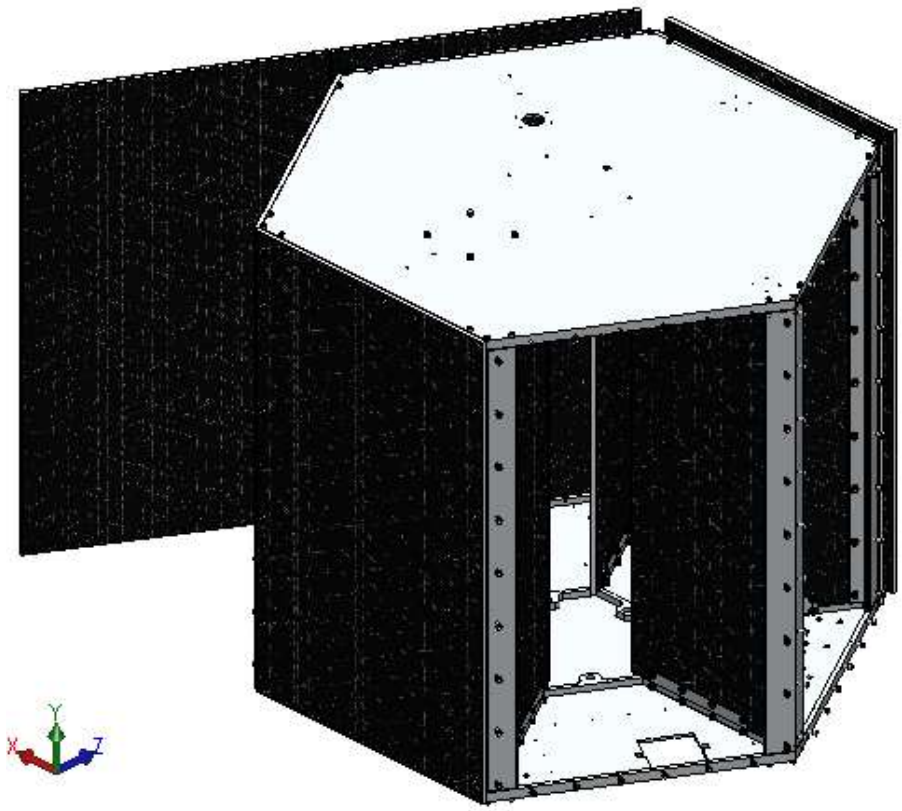

Figure 4-1. Structure isometric view

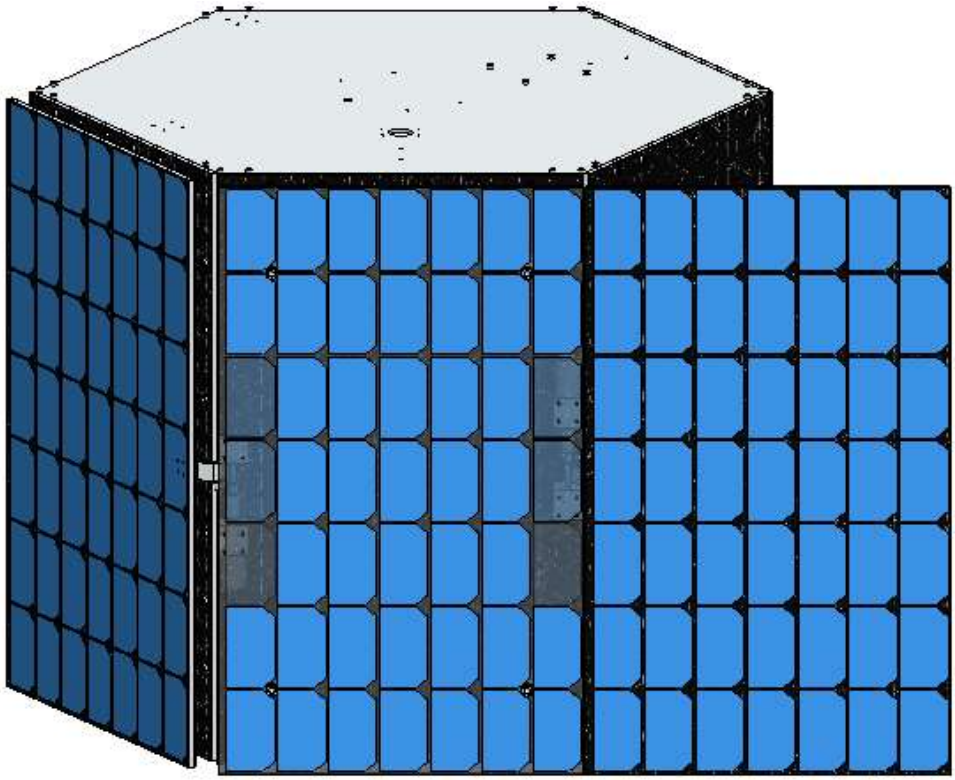

Figure 4-2. Deployable panel structure

Figure 4-3. Composite panel A

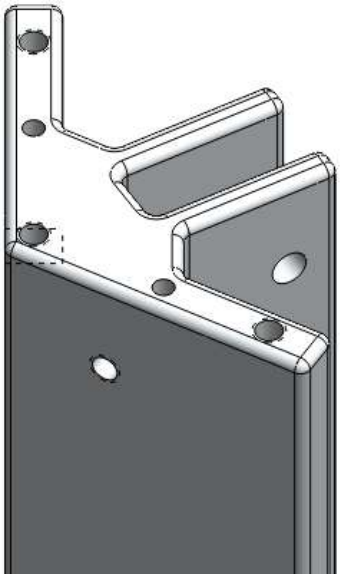

Figure 4-4. Longeron design

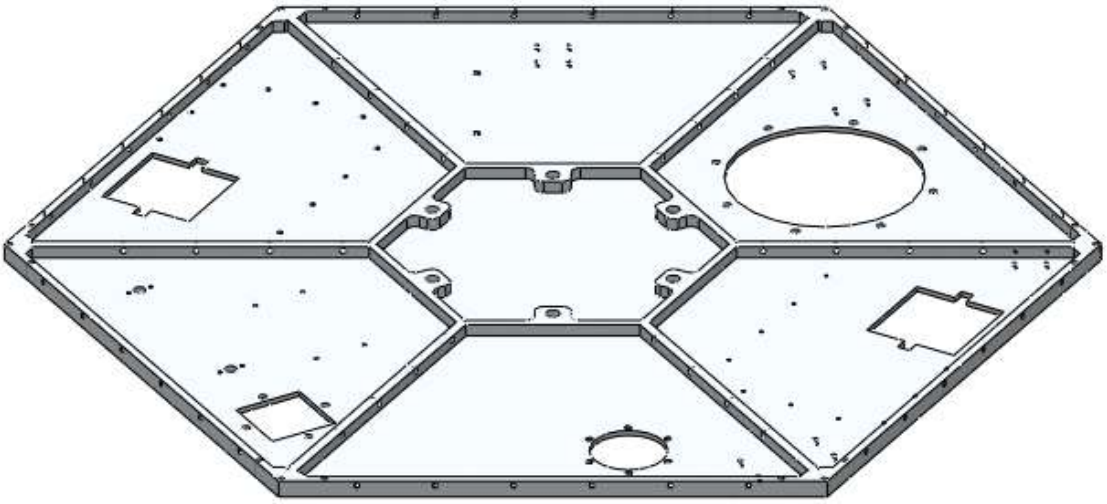

Figure 4-5. Nadir hexagon panel

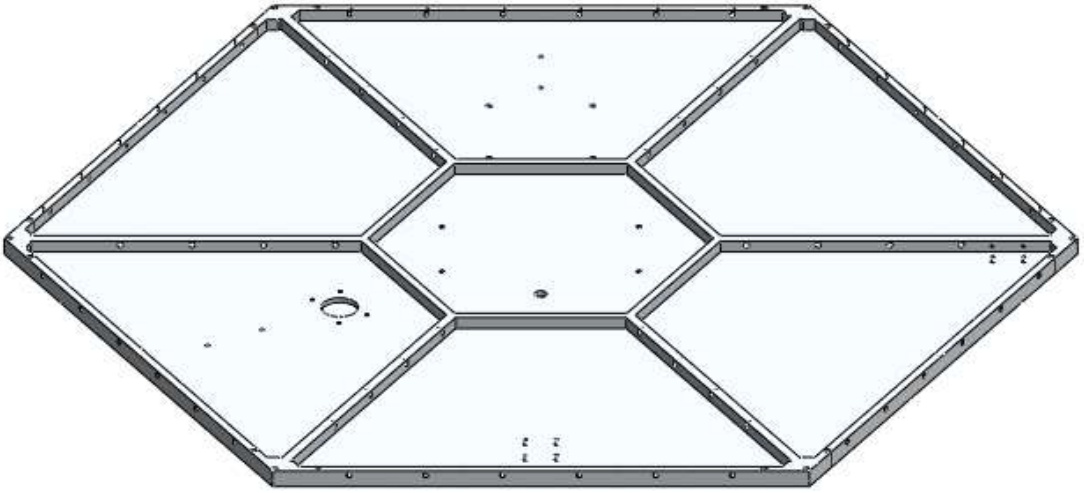

Figure 4-6. Zenith hexagon panel

Figure 4-7. Rib mounting brackets

Figure 4-8. Composite rib assembly

A 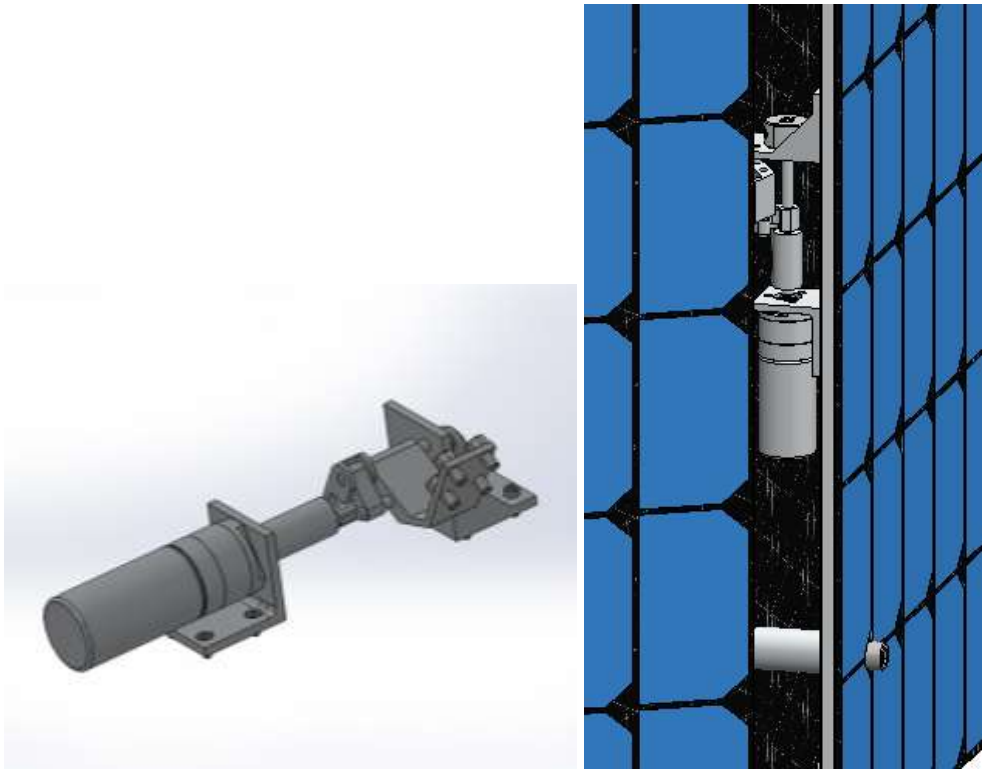 B

Figure 4-9. Deployment mechanism. A) shown in stowed and unlocked position B) shown integrated with the solar panels

CHAPTER 5
ATTITUDE DETERMINATION AND CONTROL SYSTEM

Assumptions

The following assumptions were applied to the ADCS design:

- 3-axis attitude determination and control is the most representative
- Magnetorquers are typical for LEO satellites
- Star trackers are typical for larger LEO satellites
- Gyroscopes and inertial measurement units considered equivalent
- Sun sensors are typical components for LEO satellites

Design

The attitude determination and control system (ADCS) design utilizes four sun sensors, an inertial measurement unit (IMU), a three-axis magnetometer, and two star trackers for attitude determination, four reaction wheels for three-axis attitude control, and three magnetorquer rods for detumbling. COTS spacecraft reaction wheels from Sinclair Interplanetary are shown in Figure 5-1 and are considered typical for three-axis attitude control of a small LEO satellite. Each reaction wheel has a single RS485 connector and four mounting holes [7]. Three reaction wheels provide three-axis control while the fourth reaction wheel provided redundancy. COTS Sinclair Interplanetary digital sun sensors are also shown in Figure 5-1, which are considered typical for sun detection in three orthogonal axes of a LEO satellite. Each sun sensor has a MIL-C-83513 “micro-D” connector and four mounting holes [8]. Three sun sensors are used for three-axis sun detection while a fourth provides redundancy.

A Sinclair magnetorquer is shown in Figure 5-2. A typical satellite design uses multiple magnetorquers to provide three-axes detumbling capabilities and to dump momentum to avoid saturation of the reaction wheels, for example. For DebriSat, three

magnetorquers are mounted on the composite ribs of the internal structure. Each Sinclair magnetorquer has a micro-D connection and eight mounting holes [9].

The Surrey magnetometer design is shown in Figure 5-3. Magnetometers are used in attitude determination. The Surrey magnetometer has a D-type DC connector and four mounting holes [10]. A single three-axis magnetometer is incorporated in the DebriSat design. A Surrey star tracker is also shown in Figure 5-3. Two orthogonal star trackers are used in DebriSat for precision attitude determination. The Surrey star tracker has four mounting holes and a dual redundant RS422/RS485 connector. It also requires two accompanying avionics boxes, one is a processor unit and the other is a control module [11].

A Micro Aerospace Solutions (MAS) IMU (without enclosure) is shown in Figure 5-4. IMUs are typically combined with sun sensors, horizon sensors, and star trackers to provide a complete small satellite attitude determination system. The MAS IMU has two mounting holes on its enclosure and a RS485 serial connection. A single IMU with enclosure is used in the DebriSat design and is mounted near the star trackers on the nadir panel.

Component Selection

Table 5-1 shows the breakdown of components that were donated or purchased from a supplier and those that are to be manufactured. A 60 mNm-sec reaction wheel was donated by Sinclair along with three torque rod cores. Three additional reaction wheels will be emulated based on the reaction wheel donated from Sinclair Interplanetary and three magnetorquer structures will be manufactured to incorporate the donated torque rods. A single IMU was donated by Micro Aerospace Solutions and a custom housing is required to house it. Donated components are verified for flight

quality in terms of their materials and construction. Manufactured components are based on commercially available spacecraft components such as those from Surrey Satellite Technologies and Sinclair Interplanetary to achieve representative quality.

Magnetometer

The emulated three-axis magnetometer design is shown in Figure 5-5. DebriSat will include one magnetometer mounted on panel E with multiple other ADCS components. There are four 3.5 mm diameter through holes for mounting. The enclosure is aluminum 6061 and multiple electronics boards are mounted inside.

Reaction Wheel

The design in Figure 5-6 is based on the donated Sinclair 60 mNm-sec reaction wheel. One is mounted on panel D, one on panel F, one on the nadir panel, and one on the zenith panel for a total of four reaction wheels. A ninety-degree bracket is used for the reaction wheel on the zenith panel to provide three orthogonal axes of control. The reaction wheel mounted on panel F is skewed for redundancy. Each reaction wheel uses four M2 fasteners for mounting. The emulated design uses an anodized aluminum 6061 structure, stainless steel reaction wheel, and motor driver board.

Magnetorquer

The magnetorquer housing is shown in Figure 5-7. A single torque rod core is mounted inside to complete the magnetorquer. Three magnetorquers are included in the DebriSat design to represent 3-axis magnetorquer capabilities. Eight M4 fasteners mount the magnetorquer to potted inserts in the composite ribs. One magnetorquer is parallel with the y-axis of DebriSat and the other two are skewed to provide 3-axis magnetorquer control. The enclosure and mounting clamps are anodized aluminum 6061, while the torque rod cores have been donated by Sinclair Interplanetary.

Mounting clamps provide a method for mounting the magnetorquer to the composite rib inserts. Also, four radial fasteners are at each end of the magnetorquer tube to secure the magnetorquer housing to its end caps. Lastly, the magnetorquer end cap supports a micro-d socket connector mounted directly to a 90 degree face.

Sun Sensor

Four emulated sun sensors as shown in Figure 5-8 are included in the design. Three of the sun sensors are mounted on panels A, C, and E and a fourth is mounted on the zenith panel. The emulated sun sensor uses four M2.5 fasteners for mounting, RoHS-compliant BK7 glass plano-convex lens, and an aluminum 6061 enclosure. Small light sensing electronics are mounted inside.

Star Tracker

The emulated design in Figure 5-9 is based on commercially available star trackers which typically have a baffle section and a small electronics module behind this baffle. There are four M3 mounting holes, an electronics module with an aluminum 6061 enclosure, and anodized aluminum 6061 baffle. Two star trackers are mounted orthogonal and on the nadir panel to prevent sun intrusions. The baffle is secured to the electronics module with a circular bolt pattern. A lid on the electronics module allows access to the internal light sensing electronics. Lastly, the mounting locations on the star tracker allow them to be mounted to the nadir panel in an orthogonal configuration.

ADCS Avionics

Figure 5-10 illustrates the ADCS avionics box. The box houses the electronics boards and uses multiple connectors between the flight computer and ADCS sensors and actuators. The box is mounted to panel E and uses eight M3 fasteners and the shielded enclosure is made of aluminum 6061 with a thickness of 3 mm. A 3 mm

thickness was chosen based on the performance of aluminum shielding in the AP8/AE8 radiation models as well as the desire to include a varied number of thickness in the DebriSat design. Increased thicknesses were used on more “critical” avionics such as the DebriSat flight computer. The ADCS avionics are not as critical and therefore have a lower thickness. Shielding thicknesses were also verified by a spacecraft shielding SME[3].

IMU Housing

A custom IMU housing was designed to appropriately mount and protect the donated IMU from Micro Aerospace Solutions. The new housing is made from anodized aluminum 6061 and has a removable top so that the IMU electronics can be accessed.

Summary

Table 5-2 shows the mass breakdown of the components chosen and their quantity. These components and their quantity were chosen from the ADCS trends, the target mass, and consultation with an ADCS subject matter expert (SME)[4]. The projected total ADCS mass is approximately 4.46 kg. A contingency of 10% for each mass subtotal accounts for fasteners, variations in machining, and other irregularities not accounted for in the solid models. Materials used in the ADCS subsystem include anodized aluminum 6061, stainless steel reaction wheels, and RoHS-compliant BK7 glass. Components are assembled and mounted to the DebriSat structure using socket head fasteners.

[3] Mark Johnson (Spacecraft Shielding Expert, The Aerospace Corporation), in discussion with Sheldon Clark, January 10, 2013.

[4] Andrew Tretten (Spacecraft Attitude Determination and Control Expert, The Aerospace Corporation), in discussion with author, January 12, 2012.

In the next chapter, the design and fabrication of the DebriSat propulsion system is discussed.

Table 5-1. ADCS components

Item	Supplier	Quantity
Reaction Wheel	Manufactured	4
Magnetometer- 3-axis	Manufactured	1
Torque Rod Cores	Sinclair	3
Magnetorquer Housing	Manufactured	3
Sun Sensor	Manufactured	4
Star Tracker	Manufactured	2
MASIMU02 IMU	Micro Aerospace Solutions	1
IMU Housing	Manufactured	1

Table 5-2. ADCS mass

Component	Mass Breakdown (kg)	Quantity	Mass Subtotal (kg)	Contingency (kg)
Sun Sensor	0.03	4	0.12	0.01
Star Tracker	0.13	2	0.26	0.03
Magnetometer	0.14	1	0.14	0.01
Magnetorquer	0.85	3	2.55	0.26
Reaction Wheel	0.23	4	0.92	0.09
IMU	0.13	1	0.13	0.01
ADCS Avionics	0.34	1	0.34	0.03
		TOTAL	4.46	0.44

A   B

Figure 5-1. Reaction wheels and sun sensors. A) Sinclair reaction wheels, B) Sinclair sun sensors. Source: http://www.sinclairinterplanetary.com/reactionwheels. [Accessed 13 May 2012] and http://www.sinclairinterplanetary.com/digitalsunsensors. [Accessed 13 May 2012].

Figure 5-2. Sinclair magnetorquer. Source: http://www.sinclairinterplanetary.com/torquers. [Accessed 13 May 2012].

A 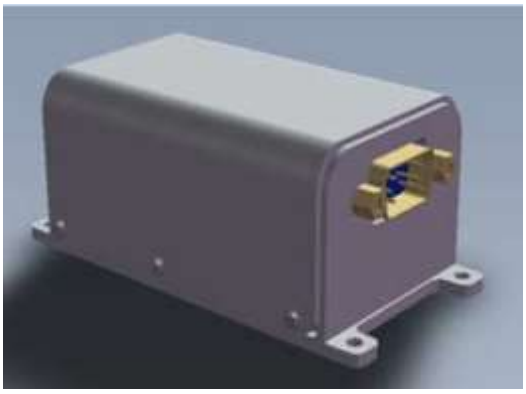 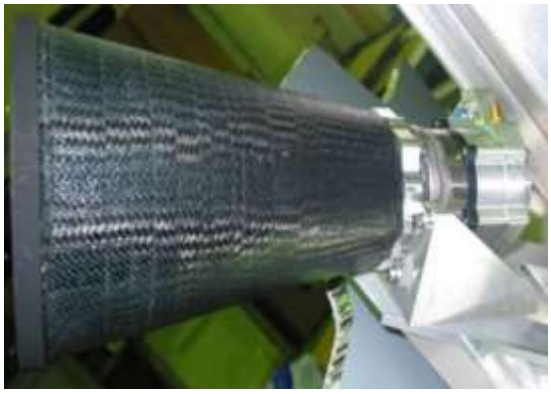 B

Figure 5-3. COTS magnetometer and star tracker. A) Surrey magnetometer, B) Surrey star tracker. Source: http://www.sstl.co.uk/Downloads/Datasheets/Subsys-datasheets/Magnetometer-ST0123582-v1-19-. [Accessed 13 May 2012] and http://www.sst-us.com/shop/satellite-subsystems/aocs/altair-hb--star-tracker--single-unit-. [Accessed 13 May 2012].

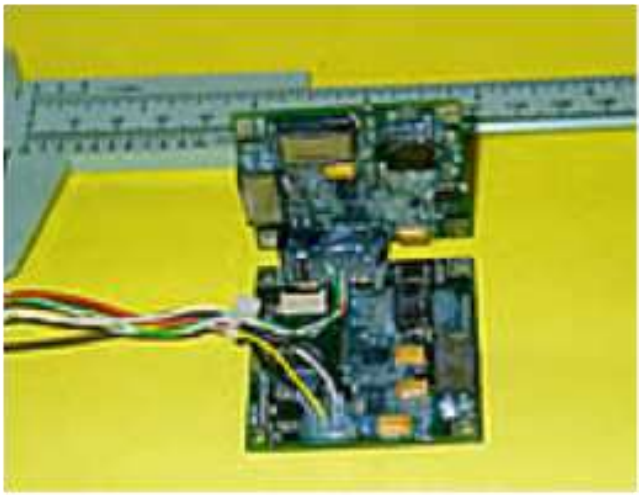

Figure 5-4. Micro Aerospace IMU. Source: http://www.micro-a.net/imu.php. [Accessed 2 August 2012].

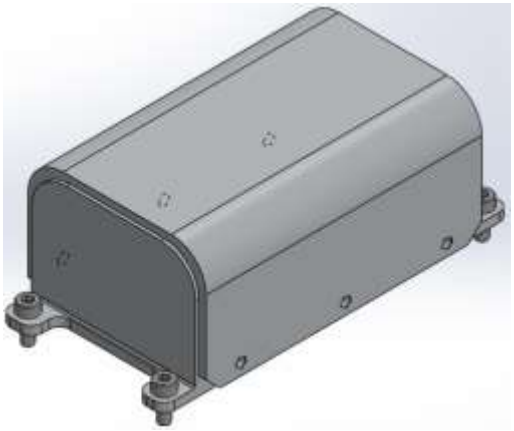

Figure 5-5. Magnetometer

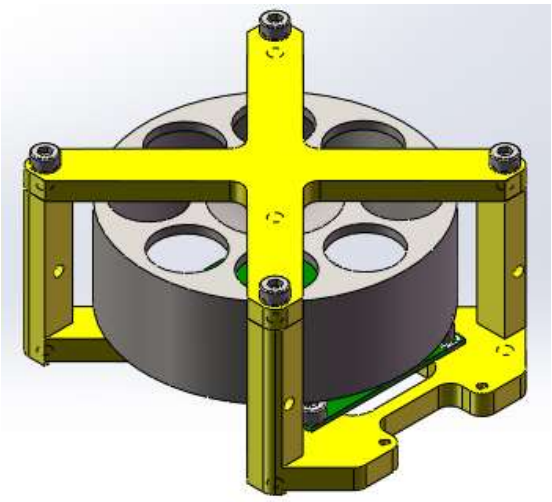

Figure 5-6. Reaction wheel

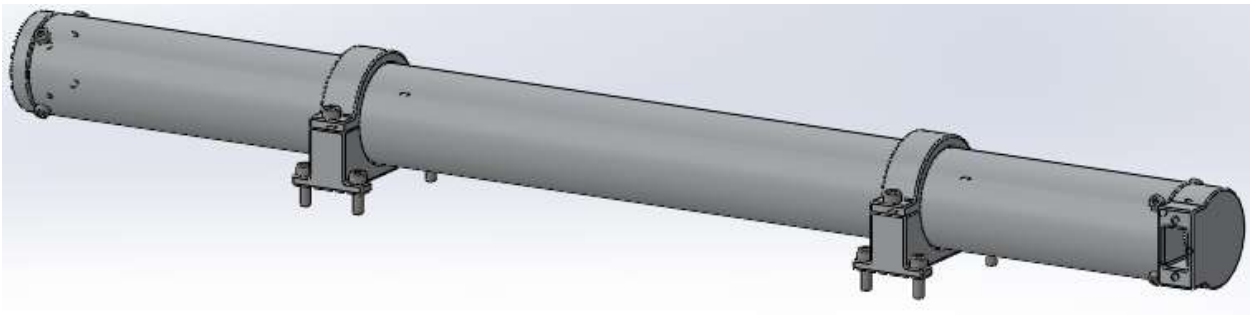

Figure 5-7. Magnetorquer

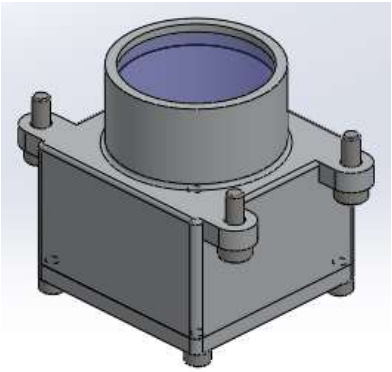

Figure 5-8. Sun sensor

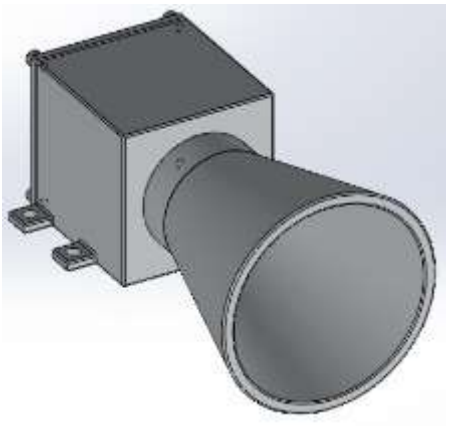

Figure 5-9. Star tracker

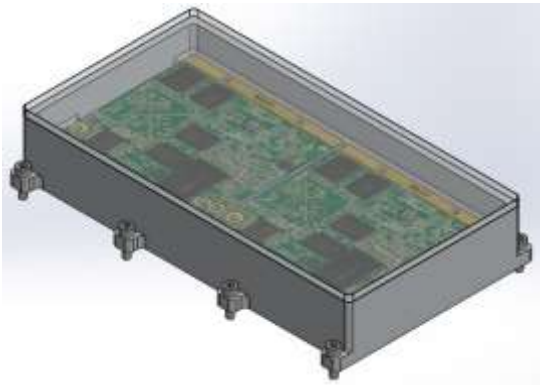

Figure 5-10. ADCS avionics

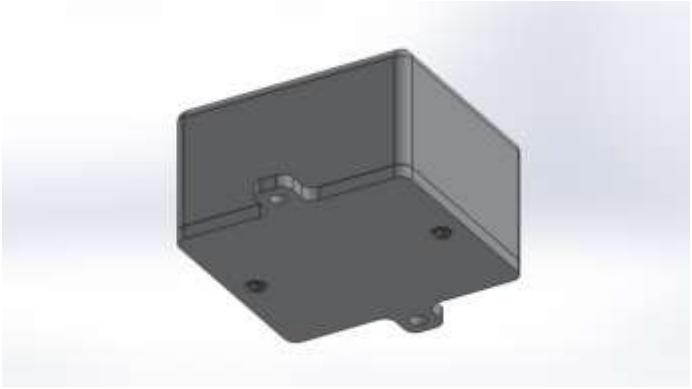

Figure 5-11. IMU housing

CHAPTER 6
PROPULSION SYSTEM

Assumptions

The DebriSat propulsion system is based on the following assumptions:

- Propulsion systems are uncommon in small LEO satellites but typical for LEO satellites in general
- The propulsion system is near “end-of-life” and therefore there is no remaining propellant
- Composite overwrapped pressure vessels (COPVs) are typical
- Central positioning of the propellant tank within a satellite is typical
- Typical components are a fuel tank, solenoids, thrusters, electronics, brackets, and plumbing
- 3-axis propulsion capability is the most typical
- Rigid metal plumbing is more representative than flexible hosing

Design

The DebriSat propulsion system utilizes six emulated thrusters, 6.35 mm stainless steel tubing, a COPV, a fill and drain valve (FDV), solenoids, and an emulated propulsion avionics unit. Three stainless steel tee-branches are utilized and all plumbing connections are welded. Plumbing follows the inside corners and faces of the structural panels and are secured to structural panels using standoffs, with approximately 46 cm spacing where possible. The COPV uses a space-qualified fiber, T1000, wrapped around an aluminum liner and is a commercial off-the-shelf (COTS) component available from HyPerComp Engineering. The base of the tank is mounted to the nadir panel using a custom mounting bracket and bonded ring. A secondary mounting bracket uses radial struts secured to the composite ribs near the valve end of the tank while

each thruster is mounted directly to the outside of the DebriSat structural panels. The integrated DebriSat propulsion system is shown in Figure 6-1.

The plumbing connections from the fuel tank, solenoids, and thrusters are shown in Figure 6-2. Thruster pairs are orthogonal to emulate propulsion capability in three axes. The fuel tank is connected to the solenoids using 6.35 mm stainless steel tubing with a wall thickness of 1.24 mm. Leaving the solenoids, three additional lines of 6.35 mm stainless steel tubing are split using stainless steel tee-branches and connect to the six thrusters. In addition to solenoid valves at the end of each thruster, there are three in-line solenoids after the electronics unit, one for each thruster pair. The diagram illustrates that a FDV allows pressurization of the COPV but that the remaining plumbing is isolated so that the solenoids and thrusters are never pressurized. In total, there is 360 cm of plumbing required.

In designing the representative propulsion system, the Surrey microsatellite gas propulsion system was considered due to its small size and mass which make it ideal for use on a 50 kg satellite. The Surrey system uses a titanium propellant tank, four experimental cold gas generators, a mounting plate, and a single resistojet thruster [13]. However, the cool gas experiment (COGEX) generators are specific to the Surrey design and would not necessarily be expected to be representative of LEO satellites. Therefore, cold gas generators are not considered in the DebriSat design. The Surrey microsatellite gas propulsion system is shown in Figure 6-3.

It was found that commercial nitrous oxide injection kits for automobiles contained many typical propulsion system components. The Zex nitrous oxide kit is shown in Figure 6-3 and has an aluminum propellant tank, flexible stainless steel

braided hoses, stainless steel fittings, a shielded electronics unit, injection nozzle, and two solenoids [14]. However, the aluminum tank in the Zex kit is too large for DebriSat and after review with a spacecraft propulsion SME , aluminum-lined COPVs are considered more representative and therefore used in the design[5].

The flexible hoses were considered for inclusion in the design, however, it was determined that rigid stainless steel pipe lines would be more representative. The electronics unit from the Zex kit is a Nitrous Management Unit (NMU) and has its own enclosure. However, the enclosure is thin-walled stainless steel which would not be considered representative of LEO satellite systems. Inside the NMU, there are solenoids that can be used for controlling flow to thrusters. Zex also sells injection nozzles that that are intended for use with their flexible hosing. However, the injection nozzle is similar to the dispersion nozzles inside resistojet thrusters and therefore was included in the DebriSat thruster design.

Component Selection

The COPV tank is obtained from an outside vendor, while the mounting brackets and thrusters require custom fabrication. Table 6-1 lists the DebriSat propulsion system components and their sourcing.

Thrusters

The thruster design is illustrated in Figure 6-4, is representative of commercially available monopropellant thrusters such as those from Surrey and Aerojet. The emulated thruster uses a Zex injection nozzle to serve as a dispersion nozzle that is

[5] Geoffrey Reber (Spacecraft Propulsion Expert, The Aerospace Corporation), in discussion with author, December 19, 2011.

typical of resistojet thrusters. The remaining components of the thruster design are: a reaction tube with nozzle, thermal shell, mounting bracket, and solenoid valve. The reaction tube is meant to withstand internal temperatures as inert gas is heated (and typically diffused) using a heater wire. The thermal shell resists heat transfer towards the spacecraft, as well as increases the surface area for radiating heat. In this design, the thermal shell provides the rear face of the reactor chamber and has through holes for mounting to the thruster mounting bracket. The solenoid valve controls flow into the thruster and is emulated using copper wire wound a stainless steel tube. While some thruster designs include the use of higher temperature bearing materials such as iridium and rhenium, the DebriSat thrusters are to be made completely of stainless steel 316L, which is typical of resistojet thrusters[6]. Also, the complicated curvature geometry of the thruster nozzle has been declared as having an insignificant effect on the potential debris fragment results and therefore may be excluded as a cost saving measure. The solenoid valve has a 6.35 mm clearance hole so that plumbing can be welded to it.

Composite-Overwrapped Pressure Vessel

The COPV is 305 mm tall with a 110 mm OD, an aluminum liner, and is wrapped with T1000 fiber (a T1000 material data sheet is provided in Appendix). It is a commercially available unit from HyPerComp Engineering [15]. The COPV uses a primary and secondary mounting bracket for mounting to the DebriSat structure. The primary and secondary mounting brackets are shown in Figure 6-5 as they would be integrated with the COPV. The primary mounting bracket is bonded to the base of the COPV with a bonding ring and uses a circular bolt pattern to mount to the nadir panel.

[6] Geoffrey Reber (Spacecraft Propulsion Expert, The Aerospace Corporation), in discussion with author, December 17, 2012.

The secondary mounting bracket is near the valve end of the COPV and uses six radial struts to secure the COPV to the composite ribs. The tank mounts to the base plate using two socket cap fasteners and is made of aluminum 6061.

Fill and Drain Valve

The addition of a functional FDV was necessary to accommodate a small amount of pressurization in the COPV. Initially, spacecraft-specific FDVs from Moog and Ad Astrium were considered for their representatives such as the one shown in Figure 6-6.

Space-qualified FDVs proved prohibitively expensive, though, so a flight-rejected valve was sought at reduced cost. However, manufacturers have been unable to supply a flight-rejected FDV. Therefore, an emulated FDV was devised that is capable of supporting pressurization. The emulated valve consists of a low-profile type 316 stainless steel ball valve available from McMaster-Carr which offers ¼ NPT male threads on both ends. A butt weld adapter is used on one end so that the FDV can be welded to the propulsion plumbing while an AN threaded adapter is added on the other end to facilitate filling at the AEDC test range before impact. The propulsion SME has stated that while such an emulated FDV may be longer than a typical spacecraft FDV, the resulting debris should be unaffected because the FDV is expected to remain intact due to its strong and compact stainless steel construction and because it will be protruding from the side of a panel[7]. The proposed McMaster-Carr valve is shown in Figure 6-7.

[7] Geoffrey Reber (Spacecraft Propulsion Expert, The Aerospace Corporation), in discussion with author, December 17, 2012.

Propulsion Avionics

An emulated propulsion avionics box was designed in lieu of using the Zex NMU since the thin stainless steel shielding of the NMU is not considered representative of typical satellite avionics. Therefore a custom propulsion avionics box was designed using aluminum 6061 with a shielding thickness of 3 mm as shown in Figure 6-8. While the Zex NMU contained solenoid valves internally, the propulsion avionics box will not include solenoid valves. Instead, the solenoid valves will be located along the plumbing lines external to the avionics box.

Plumbing Standoffs

A standoff has been designed to secure the propulsion plumbing to the wall of DebriSat. The standoffs are mostly employed near the ends of the plumbing to provide additional strength near welded areas and also to secure lengthy sections of plumbing. The standoff is a clamp based design as shown in Figure 6-9. The standoff is made of aluminum 6061 and accommodates a 6.35 mm outer diameter (OD) tube.

Solenoids

Three in-line solenoid valves are placed along the DebriSat plumbing routes external to the propulsion avionics which was confirmed by a spacecraft propulsion SME to be a representative approach[8]. A COTS solution was first sought for the solenoid valve, however the COTS options found typically included a plastic housing which would not be representative of spacecraft solenoids. Therefore, an emulated solenoid was designed from stainless steel 316L with two threaded ports for butt weld adapters and a copper winding inside.

[8] Geoffrey Reber (Spacecraft Propulsion Expert, The Aerospace Corporation), in discussion with author, January 29, 2013.

Summary

Table 6-2 lists the estimated masses for each component in the propulsion system design. Masses for the propellant tank, mounting brackets, plumbing, avionics, and thrusters were estimated using SolidWorks models and specifying material properties for each component. Mass for the dry nitrous nozzle was provided by Zex. Plumbing was calculated based on length by SolidWorks and therefore the quantity is specificed as N/A and treated as one. Plumbing includes the mass of tubing and fittings. A 10% contingency was added for all mass subtotals to account for the mass of fasteners, variations in machining, and irregulatarities not accounted for in the SolidWorks models. Materials used in the propulsion system include aluminum for mounting brackets, base plate, and propellant tank, stainless steel for fasteners, fittings, tubing, and thrusters, carbon fiber for the COPV, and copper in the solenoid valves. High-temperature bearing materials are not included in the thruster design because stainless steel is considered representative for resistojet thrusters.

In the next chapter, the DebriSat design and fabrication of the DebriSat thermal management system is discussed.

Table 6-1. Propulsion components

Component	Supplier	Quantity
COPV Tank (11.4 cm OD and 29.2 cm height)	HyPerComp	1
Propulsion Avionics	Manufactured	1
Dry Nitrous Nozzle	Zex	6
Primary Mounting Bracket	Manufactured	1
Secondary Mounting Bracket	Manufactured	1
6.35 mm Tube (1.83 m long ea.)	McMaster	3
6.35 mm Branch Tee	McMaster	6
Thruster	Manufactured	6
In-line Solenoid	Manufactured	3

Table 6-2. Propulsion component masses

Component	Mass (kg)	Quantity	Mass Subtotal (kg)	Contingency (kg)
COPV	0.77	1	0.77	0.08
Primary Mount	0.30	1	0.30	0.03
Secondary Mount	0.30	1	0.30	0.03
Plumbing	0.10	N/A	0.10	0.01
Thruster	0.30	6	1.80	0.18
Solenoid Valve	0.12	3	0.36	0.04
Standoff	0.01	8	0.08	0.01
Propulsion Avionics	0.39	1	0.39	0.04
		TOTAL	4.10	0.42

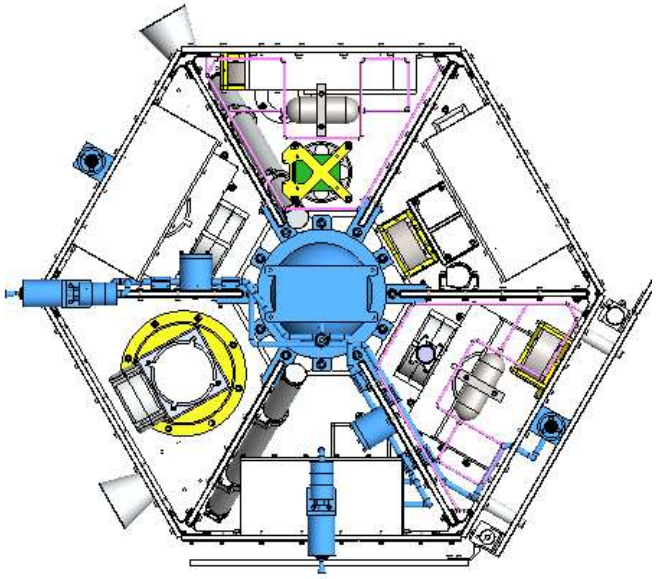

Figure 6-1. Integrated DebriSat propulsion system

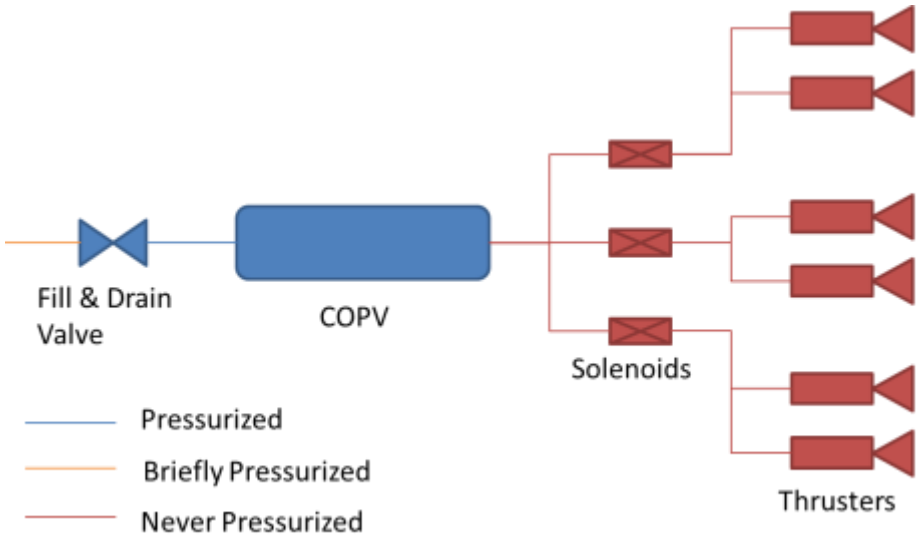

Figure 6-2. Propulsion plumbing diagram

A B

Figure 6-3. COTS propulsion system and nitrous injection system. A) Surrey microsatellite propulsion system, B) Zex nitrous fuel injection kit. Source: http://www.sstl.co.uk/Downloads/Datasheets/Subsys-datasheets/Gas-Propulsion-System-ST0065932-v004-00. [Accessed 14 February 2012] and http://www.zex.com/zx/4-6-cylinder-efi-wet-nitrous-system.html. [Accessed 11 April 2012].

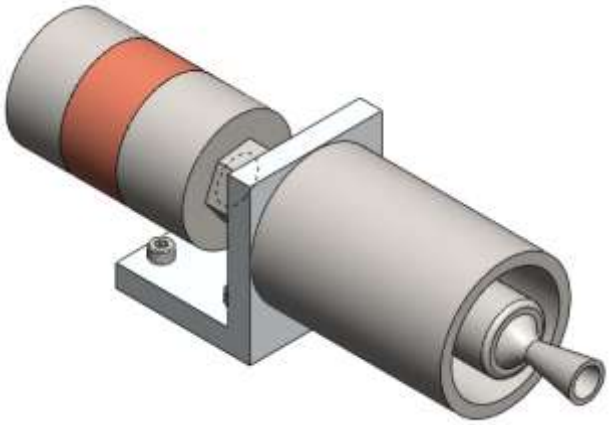

Figure 6-4. Thruster design

Figure 6-5. Composite overwrapped pressure vessel

Figure 6-6. Moog's high pressure fill and drain valve. Source: http://www.moog.com/products/propulsion-controls/spacecraft/components/fill-drain-valves/high-pressure-fill-drain-valve/. [Accessed 12 December 2012].

Figure 6-7. Low-profile ball valve. Source: http://www.mcmaster.com/#45395K101. [Accessed 17 December 2012].

Figure 6-8. Propulsion avionics

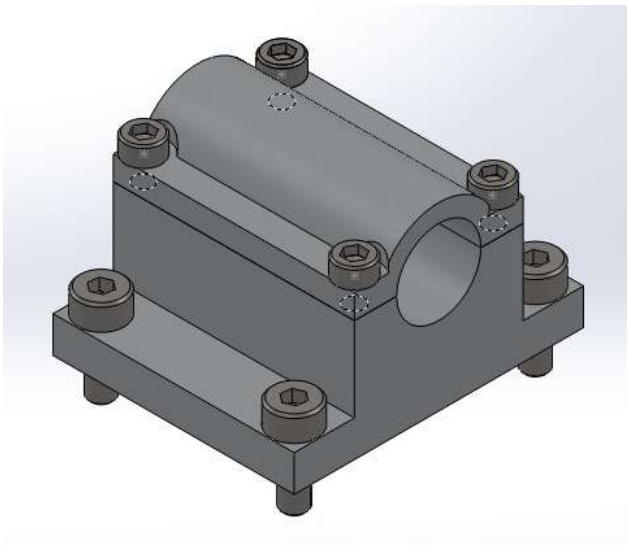

Figure 6-9. Plumbing standoff

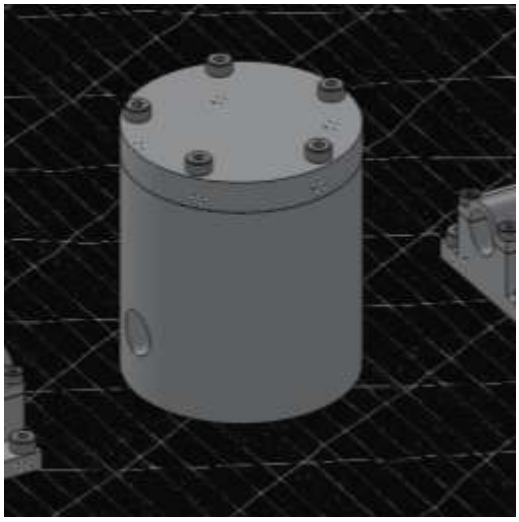

Figure 6-10. Solenoid

CHAPTER 7
THERMAL MANAGEMENT SYSTEM

Assumptions

The following assumptions are used in the thermal management design:

- Capillary pumped loop (CPL) designs are typical
- Heat pipes are required only where radiation heat transfer is not sufficient
- The absence of working fluid will not affect debris fragment results
- A zenith structural panel is a suitable radiator
- Stainless steel is typical for plumbing, fittings, and reservoirs
- Multi-layer insulation (MLI) is typical for the external faces
- Kapton heaters are used on the majority of electronics boxes

Initially, a completely passive thermal control design was desirable for DebriSat which would incorporate heat pipes and MLI, hence the CPL design. However, Kapton heaters were added to the design since they are a common element of spacecraft thermal control based upon discussions with a spacecraft thermal control subject matter expert (SME)[9].

Design

The DebriSat thermal management system is based on CPL designs. This design would theoretically use a working fluid such as ammonia to move heat from the evaporator section (near heat-generating components) to the condenser section (radiator panel). In this case, side panels of DebriSat with heat-generating components (i.e. the flight computer and regulator box) are mounted near the evaporator and heat pipes running along the zenith hexagon panel are used as the condenser section. No working fluid will actually be used inside the pipes because it is assumed to have little effect on resulting debris fragments and could potentially contaminate the resulting

[9] Jeff Cha (Spacecraft Thermal Control Expert, The Aerospace Corporation), in discussion with author, April 12, 2012.

debris fragments. Figure 7-1 shows the thermal system model for a single bay and shows one of the thermal systems as it would be integrated into bay 6.

DebriSat utilizes its zenith hexagon panel as a radiator since it would theoretically face deep space most of the time, hence the triangular segment of heat pipes that is in the bottom of Figure 7-1. The rectangular vertical plane of pipes in the same figure is internally laid in the composite side panels to extract heat from components mounted there, serving as the evaporator section. The CPL is designed to integrate into a single bay. In DebriSat, two CPLs are integrated, one in bay 6 and the other in bay 4. This is because the flight computer box in bay 4 and the battery regulator box in bay 6 are both mounted a distance from the radiator panel on the zenith face, requiring heat pipes to facilitate the transfer of heat to the radiator.

Figure 7-2 illustrates the two CPL thermal systems as they would be mounted to the radiator (zenith panel). Cutout sections in the zenith panel are utilized by the condenser segments of plumbing. Plumbing in the condenser section follows along the grooves of the zenith panel and attempts to equally distribute plumbing along an entire bay section in the panel. Since the majority of the CPL is integrated into a composite panel, standoffs are not used.

MLI with 10 layers is planned for use on the external surface area of DebriSat (except the radiator panel); this surface area is estimated in Table 7-1 from SolidWorks CAD models. The amount of thermal insulation needed is then estimated by assuming an optimal MLI density of 22 mg/cm^2 (from the Dunmore material data sheet found in Appendix). The resulting mass of MLI is calculated as 0.25 kg. The selected MLI is 25 ga polyester aluminized on one side and crinkled with 26 layers per cm. While thermal

paints were considered, none will be included because color-coding of different regions of DebriSat is planned to assist with the post-impact analysis of debris fragments.

Kapton heaters are utilized along the side panels and on electronics boxes as would typically be done to maintain internal satellite temperatures during thermal cycles experienced on orbit. The amount of Kapton needed is estimated in Table 7-2. The required surface area is what would be needed to cover many of the electronics boxes. This is estimated as roughly 1000 cm^2 which is less than 25% of the internal surface area of the side panels themselves, since electronics boxes account for a minor percentage of total side panel surface area and Kapton heaters are not required to cover the entire surface area of an electronics box.

Component Selection

The components for the thermal system and their sourcing are listed in Table 7-3. Most components in the design are COTS and can be purchased from McMaster-Carr. The CPL reservoir however, is a small stainless steel pressure vessel and would require custom fabrication. 3.175 mm OD stainless steel tubing with a wall thickness of 1.24 mm is used for all heat pipes. All plumbing connections are welded. Flexible polyimide film Kapton heaters of 0.127 cm (5 mils) thickness and various lengths and widths are available from Omega Engineering.

Kapton Heaters

The selected Kapton heaters are 0.127 cm thick (5 mils) and material properties are based on DuPont Kapton HN general-purpose polyimide film (data sheet in Appendix). Wiring harnesses for Kapton heaters will be included and will be shielded with either Kevlar or braided stainless steel sleeves.

CPL Reservoir

The emulated CPL reservoir design is made out of stainless steel 316, is 29 mm in diameter, and is 92 mm long. There are two 3.125 mm clearance holes on each end for welding to stainless steel 316 inlet and outlet pipes. Reservoir designs are typically oversized such that a void always exists within it. This makes the device operate in a variable-conductance mode, wherein the temperature of the thermally remote reservoir controls the evaporator temperature, and the condenser floods as needed such that the overall conductance of the device is controlled by this reservoir temperature [18]. The reservoir temperature is controlled by a local Kapton heater.

Reservoir mounting clamp

The reservoir mounting clamp is shown in Figure 7-4. The clamp uses two M5 cap screws to secure the CPL reservoir. One clamp is user per reservoir and the clamp mounts to the zenith panel using two M3 fasteners. The clamp is made of stainless steel 316L.

Summary

The masses of the thermal system components are listed in Table 7-4. It is noted that some designs use deployable radiators which would account for additional mass. However, a deployed radiator system cannot be used due to limitations of the impact test chamber. A 10% contingency was applied to all mass subtotals to account for irregularities not accounted for in the solid models. However, a 15% contingency is applied to Kapton heaters to also account for the surface area estimates for where Kapton is needed. Materials used in the thermal management system include stainless steel tubing, reservoirs, and clamps, aluminized polyester for MLI, and polyimide film for Kapton heaters.

In the next chapter, a detailed loads analysis on the DebriSat composite panels is presented which was used to determine the validity of the DebriSat composite panel designs as well as the selection of carbon fiber material.

Table 7-1. MLI surface area

Component	Surface Area (cm^2)
Side Panels	9000
Nadir Panel	2340
TOTAL	11340

Table 7-2. Kapton parameters

Parameter	Quantity	Unit
Surface Area	1000	cm^2
Thickness	0.127	cm
Volume	254	cc
Density	1.42	g/cc
Mass	0.18	kg

Table 7-3. Thermal system components

Component	Supplier	Quantity
CPL Reservoir	Manufactured	2
3.175 mm OD Tube (711 mm)	McMaster	10
3.175 mm OD to 1/8 NPT Male Fitting	McMaster	4
3.175 mm OD Coupling	McMaster	2
CPL Mounting Bracket	Manufactured	2
Standard Super Insulation	Dunmore	0.25 kg
Kapton Heaters (5 mil thickness)	Omega	1000 cm^2

Table 7-4. Thermal system component masses

Component	Mass (kg)	Quantity	Mass Subtotal (kg)	Contingency (kg)
Reservoir	0.14	2	0.28	0.03
Plumbing	0.05	N/A	0.05	0.01
Bracket	0.12	2	0.24	0.02
MLI	0.25	1	0.25	0.03
Kapton Heaters	0.36	1	0.18	0.05
		TOTAL	1.00	0.14

A 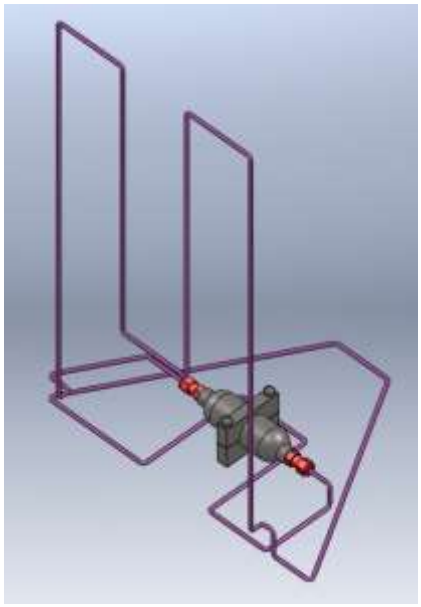 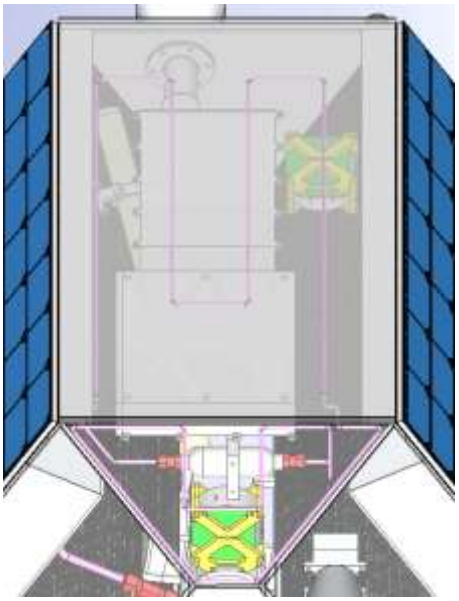 B

Figure 7-1. Capillary-pumped loop. A) CAD model for single CPL, B) CPL integrated into composite bay 6

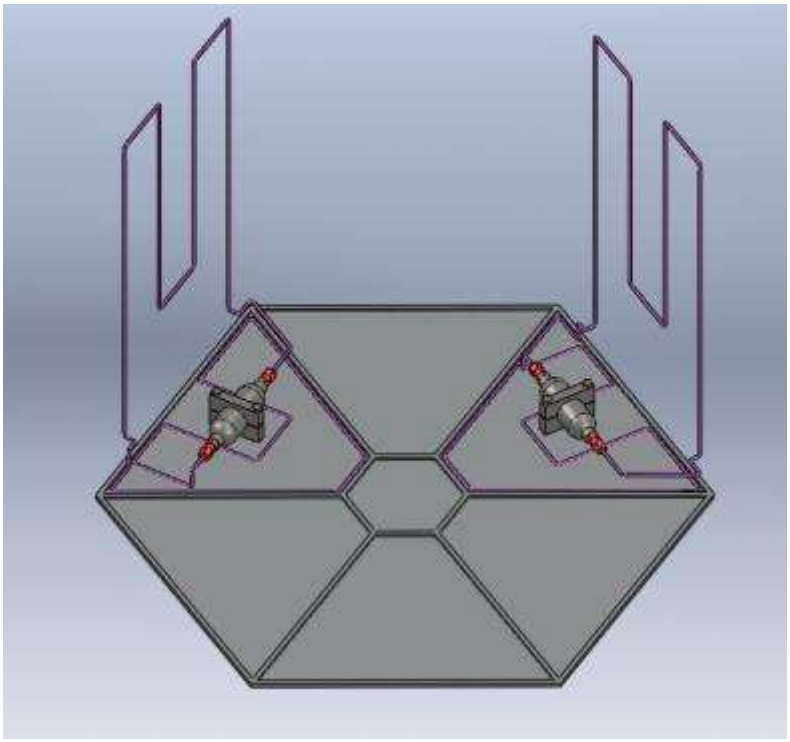

Figure 7-2. Thermal system with radiator

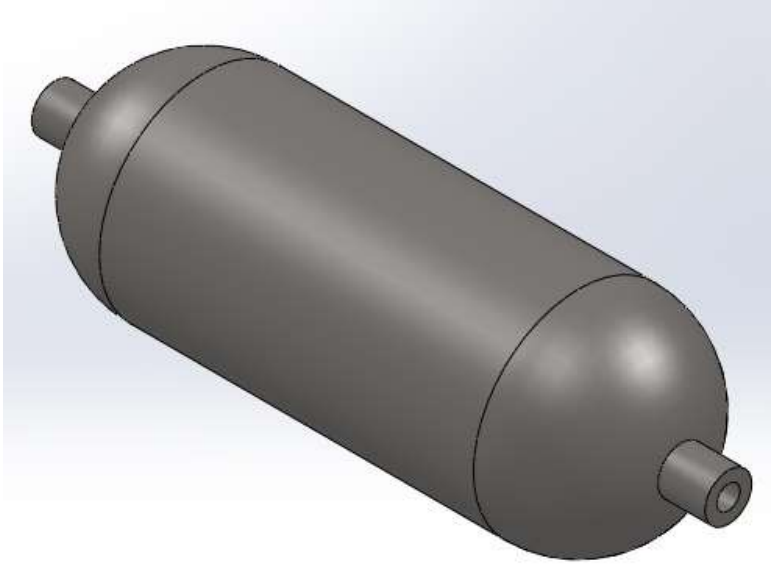

Figure 7-3. CPL reservoir

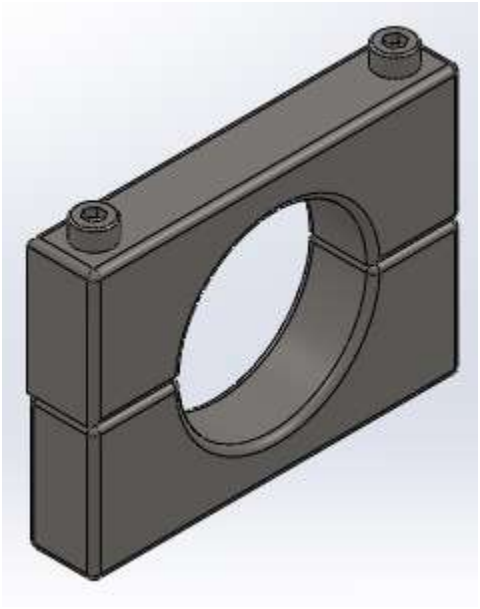

Figure 7-4. Reservoir mounting clamp

CHAPTER 8
COMPOSITES LOADS ANALYSIS

One concern during the design of DebriSat was to ensure proper selection of panel thicknesses and materials. Since the structural panels will be impacted first, any significant deviations from standard low Earth orbit (LEO) satellite panel designs could have significant effect on the resulting debris fragmentation. Therefore, the DebriSat structure was simulated under expected launch loads using a static loads analysis in SolidWorks and based on realistic launch loads expected for a primary payload. To accomplish this, the structure is subjected to simultaneous lateral and axial loading, with margin of safeties for longitudinal, transverse, and interlaminar stresses being of primary interest.

Transient and steady state accelerations chosen were based on the Minotaur IV User's Guide [19], which provided the accelerations in Table 8-1 as typical for a primary payload. The analysis was performed using the sum of transient and steady state values as recommended in the user's guide. A safety factor of 1.25 was applied.

The model used for finite element analysis (FEA) was a 2D composite shell element in SolidWorks Simulation. The model features focus on the dimensions of a single composite panel and its bolt hole connections. Complicated geometry and interactions of mounted components is excluded, except for a 4.17 kg mass distributed among bolt holes with the appropriate acceleration.

Assumptions

The following assumptions were used during the loads analysis:

- No fasteners
- Only a single composite side panel is considered
- Satellite mass is assumed as 50 kg

- Uniform distribution of satellite mass assumed across twelve composite panels
- Fixed connections are assumed along the bottom three bolt holes
- Loading on panel is evenly distributed among non-fixed bolt holes
- A safety factor of 1.25

Fasteners were removed from the model because they can be appropriately represented by loading the bolt holes. The assumption of a perfectly rigid connection along the bottom bolt holes was required since no other satellite geometry or payload adapter to support the panel is present in the model.

The mass distributed along the non-fixed bolt holes is calculated as one twelfth of the total satellite target mass of 50 kg. One twelfth is chosen because it is assumed that the total satellite mass is uniformly distributed among the six composite side panels and six composite ribs. The resulting 4.17 kg mass is applied as a remote mass at the DebriSat center of mass, assuming a rigid connection to the non-fixed bolt holes.

M46J and M55J Comparison

M55J is considered the most prevalent carbon fiber for use in space[10] and so is used as the baseline material to verify the DebriSat structure design. However, due to the difficulty of obtaining M55J fiber, M46J was considered as an alternative facesheet material due to its commercial availability, similar material properties, and because it has also been qualified for use in space previously. Therefore, an FEA simulation is also performed using M46J to ensure that it will exhibit similar breakup behavior if used as an alternative to M55J.

[10] Scott Peck (Spacecraft Structures Expert, The Aerospace Corporation), in discussion with author, April 19, 2012.

Using the safety factor of 1.25, the margin of safety (MS) is used to compare the two different fibers according to material stresses calculated inside the composite panel. The MS is calculated from:

$$MS = \frac{Strength}{Stress \times FOS} - 1$$

A visual representation of the M55J and M46J FEA setup is shown in Figure 8-1. The bottom line of mounting holes on the panel was given a fixed support while a remote mass of one twelfth of the target 50 kg was applied at the DebriSat center of gravity. The remote mass was rigidly connected to the vertical mounting holes and the top line of mounting holes. Lastly, an acceleration of 12 G in the axial (-Y) direction and 2.5 G in the lateral (-Z) direction. These loads correspond to the launch loading expected on a Minotaur IV in Table 8-1.

The material properties used in this analysis are listed in Table 8-2. M46J has a lower modulus but higher tensile strength than M55J. Most material properties were obtained from M55J and M46J data sheets available in the Appendix. Additional properties were obtained from the Toray Industries listing of functional and compressive properties [20]. Properties are defined in the local coordinate system of the composite fiber directions or ply orientations, where X is the longitudinal direction (along the ply) and Y is transverse (perpendicular to the ply). These ply directions are distinctly different from the “axial” and “lateral” directions used when discussing the applied loads on the DebriSat structure, which are in the global coordinate frame of the entire DebriSat structure.

M55J Results

Highly localized stresses were observed around the bolt hole locations of the composite and are shown with their MS in Table 8-3. Tensile (T) and compressive (C) stresses are shown. Transverse and interlaminar failures were observed, however, these were highly localized to the vicinity of the bolt holes and do not necessarily constitute a catastrophic failure.

Disregarding the highly localized stresses around the bolt hole locations, nominal stresses for the composite panel are provided in Table 8-4. From these results it is shown that the M55J is suitably designed to withstand launch loading. There is indication of transverse failure, however, this is not necessarily undesirable and so does not disqualify the panel design.

The maximum longitudinal stresses occurred at the nadir mounting hole near the corner of the panel with a maximum tensile loading of 302 MPa and a maximum compressive loading of 223 MPa. The tensile and compressive longitudinal stresses are illustrated in Figure 8-2. It is evident that the high longitudinal stresses are localized to the vicinity of the nadir bolt holes. The longitudinal stresses are well within the MS for the M55J panel. Nominal longitudinal stresses in the panel were 127 MPa for compressive and 48.2 MPa for tensile.

The maximum compressive transverse stress was 104 MPa while the maximum tensile transverse stress was 123 MPa as shown in Figure 8-3. Maximum and nominal transverse tensile stresses exceeded the MS for the M55J panel. This is expected to result in cracking in the matrix material however these transverse stresses alone do not necessarily disqualify the composite panel design according to a spacecraft structures

SME[11]. Nominal transverse stress in the panel were 47.2 MPa for tensile and 28.6 MPa for compressive.

Interlaminar shear stresses for the M55J panel are shown in Figure 8-4. It is observed that the worst case interlaminar stresses occur at the nadir bolt hole locations. While the worst case interlaminar stresses exceed the MS in highly localized regions near the bolt holes, nominal interlaminar stresses in the majority of the panel are within acceptable safety margins. Maximum stresses were 261 and 184 MPa for longitudinal and transverse interlaminar stresses, respectively.

M46J Results

Maximum stresses for the M46J panel are shown in Table 8-5. These maximums were highly localized in the vicinity of the nadir bolt holes. The material strength is exceeded in the case of transverse tensile and interlaminar shear stresses. However, since these failures are very localized to bolt hole locations, they do not necessarily constitute a catastrophic failure of the composite panel.

Nominal stresses observed for the M46J panel are shown in Table 8-6. The MS is met for the longitudinal and interlaminar shear cases; however, the tensile transverse stresses exceed the MS. Again, transverse stresses alone do not constitute a composite failure according to the SME and are therefore acceptable.

Longitudinal stresses for the M46J panel are shown in Figure 8-5. It is observed that the maximum and nominal longitudinal stresses are well with safety margins for the M46J panel with maximums of 122 and 244 MPa for tensile and compressive stresses,

[11] Scott Peck (Spacecraft Structures Expert, The Aerospace Corporation), in discussion with author, February 6, 2013.

respectively. Nominal stresses were 0.3 MPa and 122 MPa for longitudinal and transverse, respectively.

Transverse stresses in the M46J panel are shown in Figure 8-6. It is observed that the maximum and nominal stresses observed are not within safety margins. Transverse stresses alone in excess of the material strength do not constitute a catastrophic failure of the composite panel according to the SME. Maximum transverse stresses observed were 122 and 104 MPa for tensile and compressive, respectively. Nominal stresses were 46.6 and 28.5 MPa for tensile and compressive, respectively.

Interlaminar shear stresses for the M46J panel are shown in Figure 8-7. Maximum longitudinal interlaminar stresses were 261 MPa, while maximum transverse interlaminar stresses were 183 MPa, exceeding safety margins. Nominal longitudinal interlaminar stresses were 16.5 MPa, while transverse interlaminar stresses were 26.3 MPa, which were within safety margins.

Summary

The performance of the composite panel design using M55J is acceptable according to the safety margins at stress concentrations as shown in Table 8-7. Use of the M46J fiber in place of M55J would result in significant increases in longitudinal safety margins as shown while experiencing a slight decrease in transverse and interlaminar safety margins. These stresses are highly localized at bolt hole locations however and would not be expected to cause catastrophic failure of either the M55J or M46J panels. With the exception of longitudinal stresses, the M46J panel performed similarly to the M55J panel at the stress concentrations near the nadir bolt holes. Failure

to meet the MS for the tensile transverse stresses is observed; however, this does not necessarily disqualify the M55J or M46J panel[12].

The percent increase in nominal safety margins for the M55J and M46J panel are shown in Table 8-8. Increased safety margins are observed for the M46J panel in the longitudinal, transverse compression, and transverse interlaminar stresses, with tensile longitudinal safety margins increasing dramatically. Transverse tensile and longitudinal interlaminar safety margins decreased for the M46J panel. With the exception of tensile longitudinal safety margins, the M46J panels performed similarly to the M55J panel. Both panels are acceptable designs in terms of their safety margins and since M46J performed similar to M55J, it is an acceptable material to use in the event that M55J cannot be obtained.

In the next chapter, conclusions are made regarding the DebriSat subsystems that were presented as well as future work.

Table 8-1. Expected launch loads

	Axial (G's)	Lateral (G's)
Steady State	8	0.5
Transient	4	2
TOTAL	12	2.5

[12] Scott Peck (Spacecraft Structures Expert, The Aerospace Corporation), in discussion with author, February 6, 2013.

Table 8-2. M55J/M46J property comparison

Property	M55J Value	M46J Value	Units
Elastic Modulus in X	340000	265000	MPa
Elastic Modulus in Y	6400	7100	MPa
Poisson's Ration in XY	0.87	0.87	N/A
Poisson's Ration in YZ	0.3	0.3	N/A
Poisson's Ration in XZ	0.3	0.3	N/A
Shear Modulus in XY	3900	3900	MPa
Mass Density	1630	1590	kg/m^3
Tensile Strength in X	2010	2210	MPa
Tensile Strength in Y	34	47	MPa
Compressive Strength in X	880	1080	MPa
Shear Strength in XY	44	59	MPa

Table 8-3. Localized stress-concentrations for M55J panel

	Stress (MPa)	Strength (MPa)	FoS	MS
Longitudinal (T)	223	2010	1.25	6.2
Longitudinal (C)	-302	-880	1.25	1.3
Transverse (T)	123	34	1.25	-0.8
Transverse (C)	-104	-880	1.25	5.8
Longitudinal Interlaminar	261	74	1.25	-0.8
Transverse Interlaminar	184	74	1.25	-0.7

Table 8-4. Nominal stresses for M55J panel

	Stress (MPa)	Strength (MPa)	FoS	MS
Longitudinal (T)	48.2	2010	1.25	32.4
Longitudinal (C)	-127	-880	1.25	4.5
Transverse (T)	47.2	34	1.25	-0.4
Transverse (C)	-28.6	-880	1.25	23.6
Longitudinal Interlaminar	13.7	74	1.25	3.3
Transverse Interlaminar	26.3	74	1.25	1.3

Table 8-5. Localized stress-concentrations for M46J panel

	Stress (MPa)	Strength (MPa)	FoS	MS
Longitudinal (T)	122	2210	1.25	13.5
Longitudinal (C)	-244	-1080	1.25	2.5
Transverse (T)	122	47	1.25	-0.7
Transverse (C)	-104	-1080	1.25	7.3
Longitudinal Interlaminar	261	83	1.25	-0.7
Transverse Interlaminar	183	83	1.25	-0.6

Table 8-6. Nominal stresses for M46J panel

	Stress (MPa)	Strength (MPa)	FoS	MS
Longitudinal (T)	0.3	2210	1.25	5892.3
Longitudinal (C)	-122	-1080	1.25	6.1
Transverse (T)	46.6	47	1.25	-0.2
Transverse (C)	-28.5	-1080	1.25	29.3
Longitudinal Interlaminar	16.5	83	1.25	3.0
Transverse Interlaminar	26.3	83	1.25	1.5

Table 8-7. Percent increase in stress-concentration safety margins

	M55J MS	M46J MS	% Increase in MS
Longitudinal (T)	6.2	13.5	117%
Longitudinal (C)	1.3	2.5	91%
Transverse (T)	-0.8	-0.7	-11%
Transverse (C)	5.8	7.3	27%
Longitudinal Interlaminar	-0.8	-0.7	-4%
Transverse Interlaminar	-0.7	-0.6	-6%

Table 8-8. Percent increase in nominal safety margins

	M55J MS	M46J MS	% Increase in MS
Longitudinal (T)	32.4	5892.3	18108%
Longitudinal (C)	4.5	6.1	34%
Transverse (T)	-0.4	-0.2	-54%
Transverse (C)	23.6	29.3	24%
Longitudinal Interlaminar	3.3	3.0	-9%
Transverse Interlaminar	1.3	1.5	22%

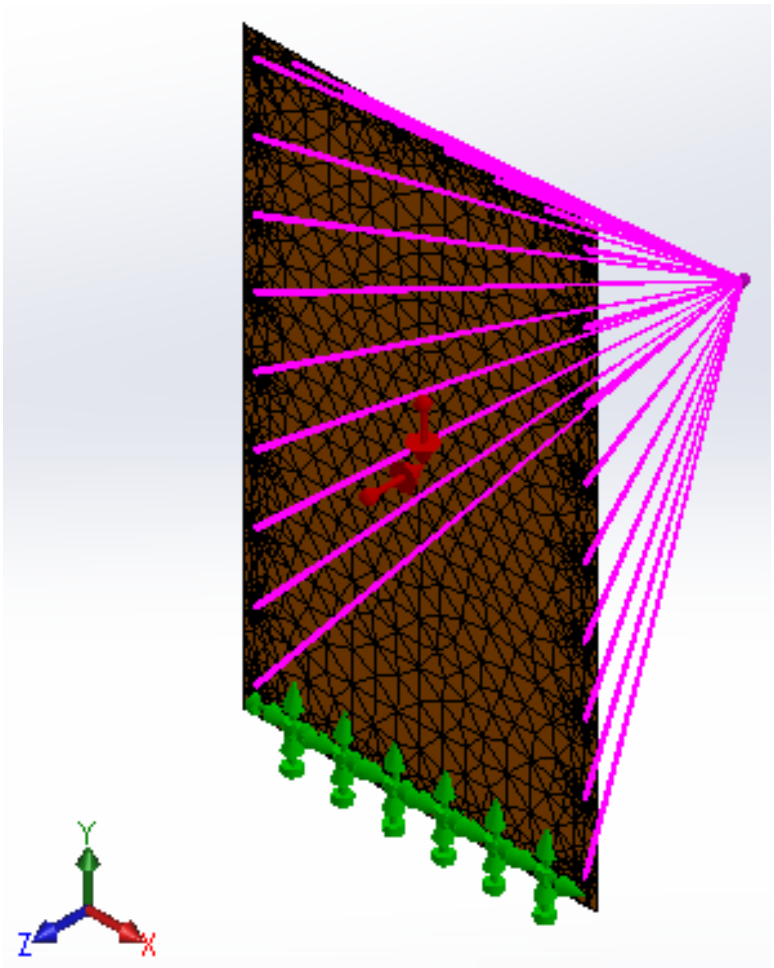

Figure 8-1. M46J/M55J FEA setup

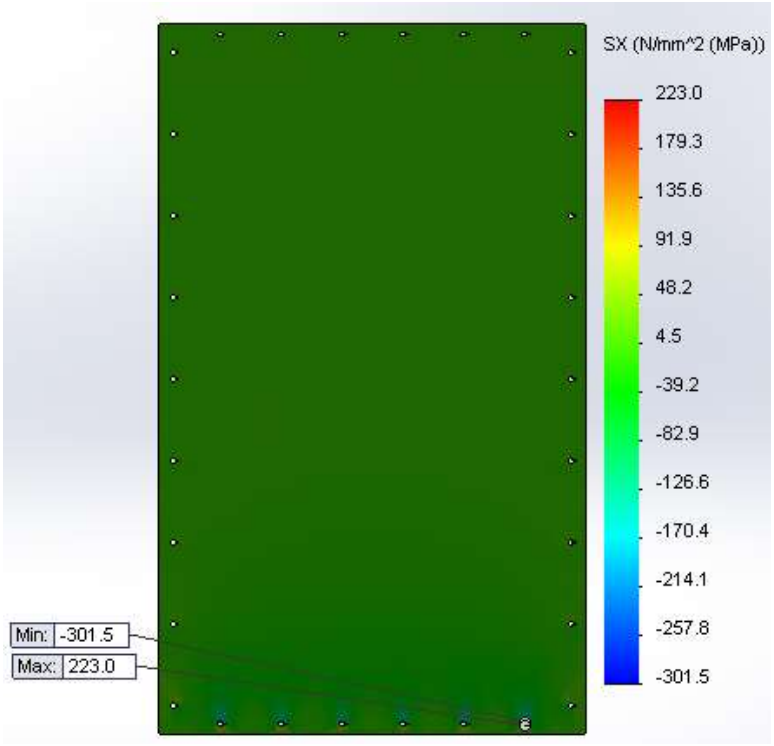

Figure 8-2. M55J longitudinal stresses

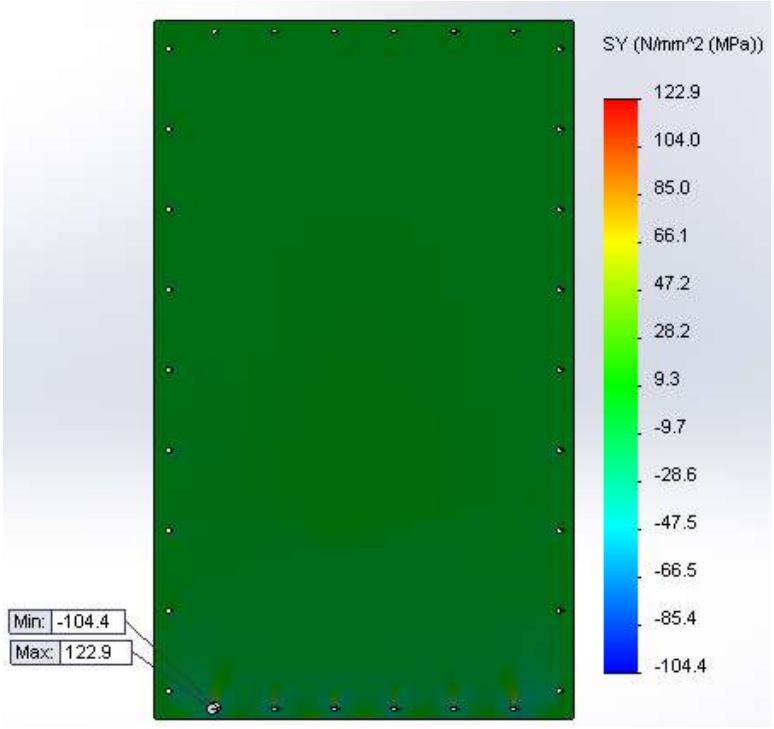

Figure 8-3. M55J transverse stresses

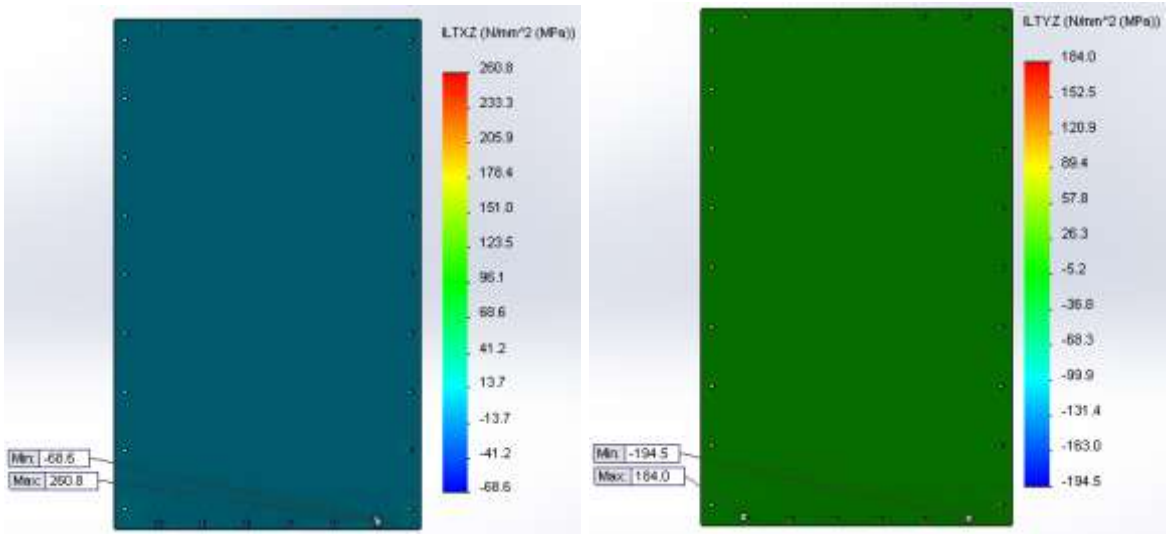

A B

Figure 8-4. M55J interlaminar shear stresses. A) longitudinal interlaminar, B) transverse interlaminar

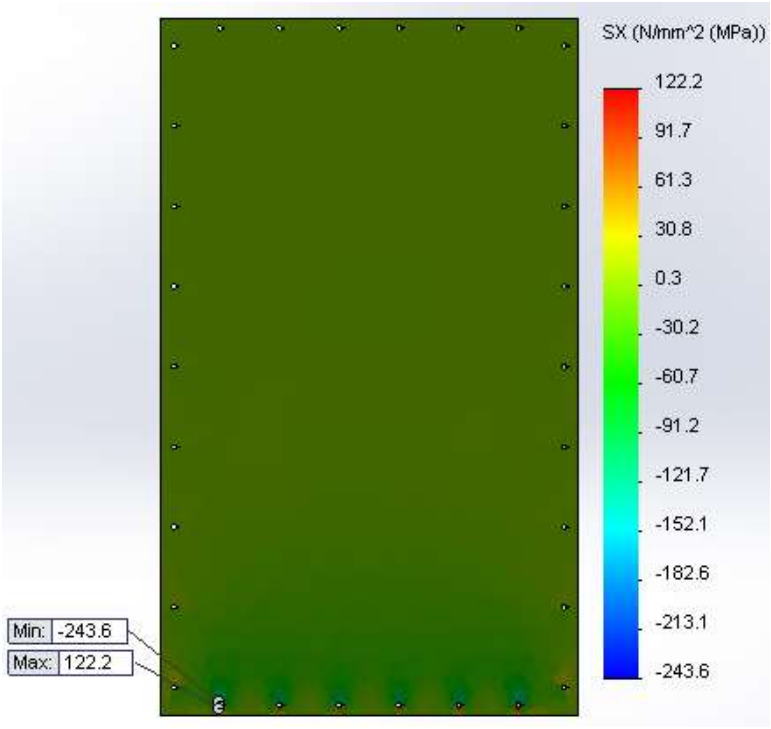

Figure 8-5. M46J longitudinal stresses

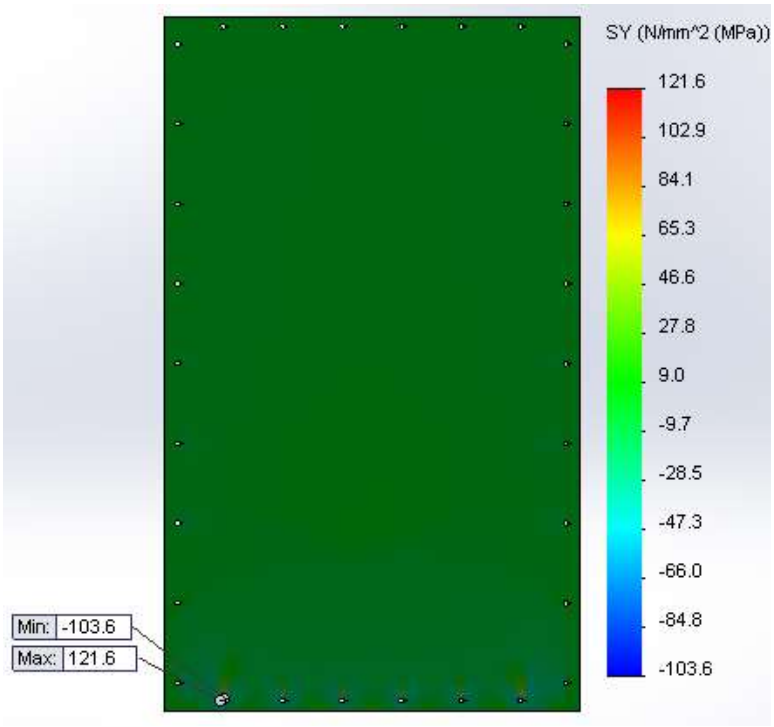

Figure 8-6. M46J transverse stresses

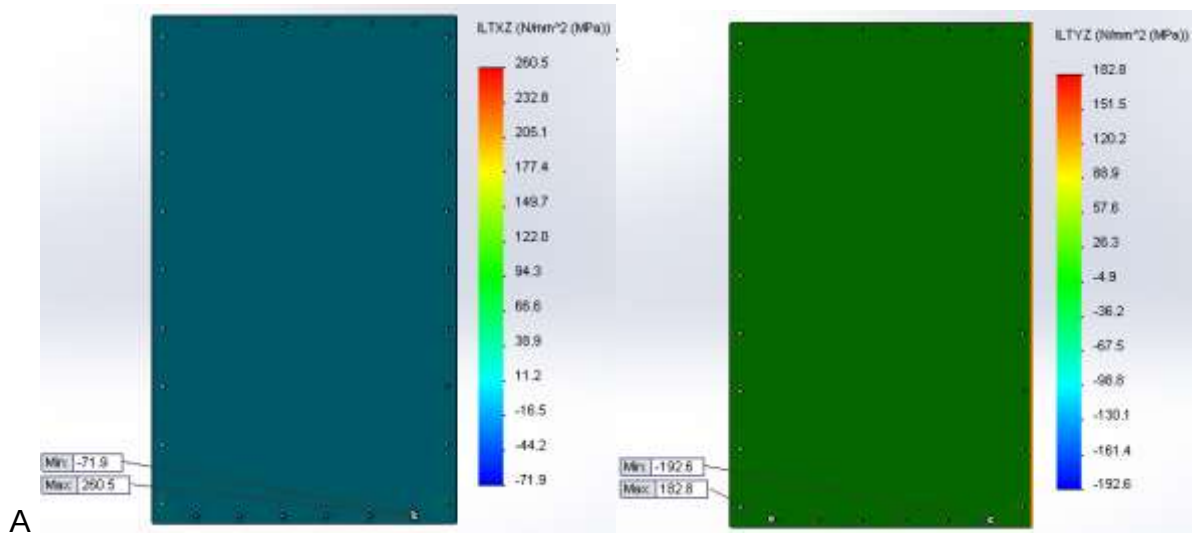

A B

Figure 8-7. M46J interlaminar shear stresses. A) longitudinal interlaminar, B) transverse interlaminar

CHAPTER 9
CONCLUSION AND FUTURE WORK

Conclusion

Representative subsystems for a modern LEO satellite were designed, specifically for structures, ADCS, propulsion, and thermal management. The materials, components, and subsystems selected are deemed representative based upon the results of a LEO satellite survey conducted by the University of Florida, observations of existing COTS spacecraft hardware, and feedback from spacecraft SMEs. While only a 50 kg satellite, DebriSat aims to represent the entire class of modern LEO satellites ranging from 1-5000 kg and therefore includes some design elements not typically expected on a 50 kg satellite platform (e.g. a propulsion system). The components presented are mostly non-functional emulations except for in a few instances such as the COPV and emulated FDV which will allow the completed DebriSat to receive a slight pressurization before the planned impact test. The subsystems presented contain major materials of interest with regards to a modern LEO satellite, specifically, composites and MLI which are included in the DebriSat structural panels, COPV, and thermal management system. Lastly, an FEA simulation is performed to validate the usage of M55J and M46J in the composite structural panels under launch loads. It is shown that both M55J and M46J are sufficient materials for use in the DebriSat structure, and also that M46J would make an acceptable alternative in the case that M55J is not obtainable.

Future Work

Representative designs for structural, ADCS, propulsion, and thermal management subsystems are presented in this thesis. The next step is to begin

obtaining and fabricating the components presented so that they can be assembled into a completed DebriSat. Small modifications to these designs may be necessary going forward to improve manufacturability. Once these components are obtained and assembled, vibrations and thermal testing will be performed. The final assembly is to be sent to the AEDC test range for the ground-based hypervelocity impact test. Efforts are currently underway to define a comprehensive test plan with the AEDC facility. After the impact, debris fragments are to be returned to the University of Florida for post-impact characterization. Efforts are also underway to develop a visual inspection system (VIS) that will expedite the debris characterization process, as well as utilize automated techniques for improved accuracy in fragment measurements. Once a sufficient quantity of debris fragments has been characterized, the results will be presented to the NASA Orbital Debris Programs Office so that improvements to the NASA standard breakup model can be made.

DUNMORE Super Insulation Technology

DUNMORE low-emissivity aluminized polyester film has become the preferred MLI in aerospace and cryogenic applications. DUNMORE Super Insulation is available in standard configurations of 25-gauge and 48-gauge, aluminized on one or both sides.

The Super Insulation Physical Properties Table details its specifications. Standard versions of DUNMORE Super Insulation are available in flat, crinkled, embossed, perforated, or porolated (needle punch) form. Custom-designed Super Insulation can be created to your unique specifications.

Physical Properties for DUNMORE Standard Super Insulation

Material	Optimum Density		Thermal Conductivity at Optimum Density	Thermal Conductivity at 15 PSI (1 kg/cm²) Compression
	mg/cm²	layers per cm	μW/cm °C	μW/cm °C
25 ga (6.3 μm) polyester aluminized on one side and crinkled	22	26	0.29	59
25 ga (6.3 μm) polyester aluminized on two sides plus:	83	19	0.19	10
• 2 layers 92 ga (23 μm) fiberglass cloth	48	20	0.08	26
• 1 layer .007 in. thickness nylon scrim	59	13	0.29	13
• 1 layer .008 in. thickness glass paper 50% perforated				
13.7 μm soft aluminum foil plus:	48	14	0.17	11
• 1 layer .003 in. thickness glass paper	80	9	0.14	6.4
• 1 layer 0.14 in. thickness glass mat				

Data from "Thermal Insulation Systems" by P. Glaser, I. Black, R. Lindstrom, Ruccia and A. Wechsler, NASA Spec. Pub. 5027 (1967)

Key Properties of Aluminum-Coated Polyester, Polyimide, and Fluorocarbon Films

	Polyester	Polyimide	Fluorocarbon	Test Methods
Physical Properties	@ 25°C (77°F)	@ 23°C (73°F)	@ 23°C (73°F)	
Density	1.40 g/cc	1.42 g/cc	2.13-2.14 g/cm³	ASTM D 1505-68
Thickness	25 gauge (6.3 microns)	100 gauge (25 microns)	200 gauge (50 microns)	DuPont® Data
Yield	576 ft²/lb	136 ft²/lb	45 ft²/lb	ASTM D 882-88
Tensile Strength	28,000 PSI/1972 kg/cm²	24,000 PSI/1690 kg/cm²	2,500 PSI/176 kg/cm²	ASTM D 882-88 (Method A*)
Thermal Properties				
Thermal Conductivity®	6.1 x 10^{-4} Watts cm^{-1} °C^{-1}	6.1 x 10^{-3} Watts cm^{-1} °C^{-1}	1.94 x 10^{-4} Watts cm^{-1} °C^{-1}	ASTM D 696
Specific Heat	.28 (cal/gm/°C)	.28 (cal/gm/°C)	.28 (cal/gm/°C)	DuPont® Data
Solar Absorptance*	≤ 0.14	≤ 0.14	≤ 0.14	ASTM E-903/E490
Emissivity*	0.035 (avg)	0.035 (avg)	0.035 (avg)	ASTM E-408 (Method A)
Service Temperature (nom.)	-250° C + 150° C	-250° C + 204° C	-150° C + 150° C	DuPont® Data
Outgassing	% TML < 1.0% %CVCM < 0.1%	% TML < 1.0% %CVCM < 0.1%	% TML < 1.0% %CVCM < 0.1%	ASTM E-595 ASTM E-595
Electrical Properties				
Resistivity, Ohms/□	< 1.0 Ω/□	< 1.0 Ω/□	< 1.0 Ω/□	DUNMORE Data
VDA Thickness Angstroms	≥ 300 Å	≥ 300 Å	≥ 300 Å	DUNMORE Data
Chemical Properties				
Moisture Absorption 50% R.H. @ 25°C (77°F)	1.0% (nominal)	4.0% (max)	1.0% (nominal)	ASTM D 570-92

Values based on 25 gauge polyester, 100 gauge polyimide, and fluorocarbon films.
* Values measured on the VDA side of the substrate.
® Values based on unmetallized films.

DuPont™ Kapton® HN

polyimide film

Technical Data Sheet

DuPont™ Kapton® HN general-purpose film has been used successfully in applications at temperatures as low as -269°C (-452°F) and as high as 400°C (752°F). HN film can be laminated, metallized, punched, formed or adhesive coated. Kapton® HN is the recommended choice for applications that require an all-polyimide film with an excellent balance of properties over a wide range of temperatures.

Applications

- Mechanical parts
- Electronic parts
- Electrical Insulation
- Pressure sensitive tape
- Fiber optics cable
- Insulation blankets
- Insulation tubing
- Automotive diaphragms sensors and manifolds
- Etching
- Shims

Product Specifications

Kapton® HN is manufactured, slit and packaged according to the product specifications listed in H-38479, Bulletin GS-96-7.

Certification

Kapton® HN meets ASTM D-5213 (type 1, item A) requirements.

DUPONT

The miracles of science™

Table 1
Physical Properties of DuPont™ Kapton® HN at 23°C (73°F)

Property	Unit	1 mil 25µm	2 mil 50µm	3 mil 75µm	5 mil 125µm	Test Method
Ultimate Tensile Strength at 23°C, (73°F) at 200°C (392°F)	psi (MPa)	33,500(231) 20,000(139)	33,500(231) 20,000(139)	33,500(231) 20,000(139)	33,500(231) 20,000(139)	ASTM D-882-91, Method A*
Ultimate Elongation at 23°C, (73°F) at 200°C (392°F)	%	72 83	82 83	82 83	82 83	ASTM D-882-91, Method A
Tensile Modulus at 23°C, (73°F) at 200°C (392°F)	psi (GPa)	370,000 (2.5) 290,000 (2.0)	370,000 (2.5) 290,000 (2.0)	370,000 (2.5) 290,000 (2.0)	370,000 (2.5) 290,000 (2.0)	ASTM D-882-91, Method A
Density	g/cc	1.42	1.42	1.42	1.42	ASTM D-1505-90
MIT Folding Endurance	cycles	285,000	55,000	6,000	5,000	ASTM D-2176-89
Tear Strength-propagating (Elmendorf), N (lbf)		0.07 (0.02)	0.21 (0.02)	0.38 (0.02)	0.58 (0.02)	ASTM D-1922-89
Tear Strength, Initial (Graves), N (lbf)		7.2 (1.6)	16.3 (1.6)	26.3 (1.6)	46.9 (1.6)	ASTM D-1004-90
Yield Point at 3% at 23°C, (73°F) at 200°C (392°F)	MPa (psi)	69 (10,000) 41 (6,000)	69 (10,000) 41 (6,000)	69 (10,000) 41 (6,000)	69 (10,000) 41 (6,000)	ASTM D-882-91
Stress to produce 5% elong. at 23°C, (73°F) at 200°C (392°F)	MPa (psi)	90 (13,000) 61 (9,000)	90 (13,000) 61 (9,000)	90 (13,000) 61 (9,000)	90 (13,000) 61 (9,000)	ASTM D-882-92
Impact Strength at 23°C, (73°F)	N•cm•(ft lb)	78 (0.58)	78 (0.58)	78 (0.58)	78 (0.58)	DuPont Pneumatic Impact Test
Coefficient of Friction, kinetic (film-to-film)		0.48	0.48	0.48	0.48	ASTM D-1894-90
Coefficient of Friction, static (film-to-film)		0.63	0.63	0.63	0.63	ASTM D-1894-90
Refractive Index (sodium D line)		1.70	1.70	1.70	1.70	ASTM D-542-90
Poisson's Ratio		0.34	0.34	0.34	0.34	Avg. three samples, elongated at 5, 7, 10%
Low temperature flex life		pass	pass	pass	pass	IPC-TM-650, Method 2.6.18

*Specimen size 25 x 150 mm (1.6 in); jaw separation 100 mm (4 in), jaw speed, 50mm/min (2 in/min). Ultimate refers to the tensile strength and elongation measured at break.

TECHNICAL DATA SHEET
No. CFA-017

TORAYCA®

M55J DATA SHEET

MJ type high modulus fiber with enhanced tensile and compressive strength over ***M*** series fibers. Mainly used for premium sporting goods, aerospace, and industrial applications.

FIBER PROPERTIES

		English	Metric	Test Method
Tensile Strength		583 ksi	4,020 MPa	TY-030B-01
Tensile Modulus		78.2 Msi	540 GPa	TY-030B-01
Strain		0.8 %	0.8 %	TY-030B-01
Density		0.069 lbs/in^3	1.91 g/cm^3	TY-030B-02
Filament Diameter		2.0E-04 in.	5 µm	
Yield	6K	6,833 ft/lbs	218 g/1000m	TY-030B-03
Sizing Type & Amount	50B	1.0 %		TY-030B-05
	Twist	Untwisted		

FUNCTIONAL PROPERTIES

CTE	-1.1 $\alpha \cdot 10^{-6}$/°C
Specific Heat	0.17 Cal/g·°C
Thermal Conductivity	0.372 Cal/cm·s·°C
Electric Resistivity	0.8 x 10^{-3} Ω·cm
Chemical Composition: Carbon	>99 %
Na + K	<50 ppm

COMPOSITE PROPERTIES*

Tensile Strength	290 ksi	2,010 MPa	ASTM D-3039
Tensile Modulus	49.0 Msi	340 GPa	ASTM D-3039
Tensile Strain	0.6 %	0.6 %	ASTM D-3039
Compressive Strength	130 ksi	880 MPa	ASTM D-695
Flexural Strength	180 ksi	1,230 MPa	ASTM D-790
Flexural Modulus	40.5 Msi	280 GPa	ASTM D-790
ILSS	10.0 ksi	7 kgf/mm^2	ASTM D-2344
90° Tensile Strength	5.0 ksi	34 MPa	ASTM D-3039

* Toray 250°F Epoxy Resin. Normalized to 60% fiber volume.

TORAY CARBON FIBERS AMERICA, INC.

M55J

COMPOSITE PROPERTIES**

Tensile Strength	270 ksi	1,860 MPa	ASTM D-3039
Tensile Modulus	43.5 Msi	300 GPa	ASTM D-3039
Tensile Strain	0.6 %	0.6 %	ASTM D-3039
Compressive Strength	120 ksi	835 MPa	ASTM D-695
Compressive Modulus	41.5 Msi	285 GPa	ASTM D-695
In-Plane Shear Strength	6.5 ksi	44 MPa	ASTM D-3518
ILSS	10.5 ksi	7.5 kgf/mm^2	ASTM D-2344
90° Tensile Strength	5.0 ksi	35 MPa	ASTM D-3039

** Toray Semi-Toughened 350°F Epoxy Resin. Normalized to 60% fiber volume.

See Section 4 for Safety & Handling information. The above properties do not constitute any warranty or guarantee of values. These values are for material selection purposes only. For applications requiring guaranteed values, contact our sales and technical team to establish a material specification document.

PACKAGING

The table below summarizes the tow sizes, twists, sizing types, and packaging available for standard material. Other bobbin sizes may be available on a limited basis.

Tow Sizes	Twist[1]	Sizing	Bobbin Net Weight (kg)	Bobbin Type[2]	Bobbin Size (mm) a	b	c	d	e	Spools per Case	Case Net Weight (kg)
6K	B	50B	0.5	II	76	82	192	107	156	24	12

[1] **Twist** A: Twisted yarn B: Untwisted yarn made from a twisted yarn through an untwisting process C: Never twisted yarn

[2] **Bobbin Type** See Diagram below

TYPE I

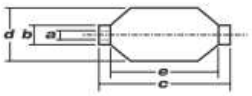

TYPE II

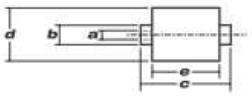

TYPE III

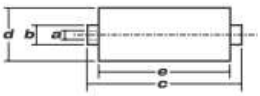

TORAY CARBON FIBERS AMERICA, INC.
6 Hutton Centre Drive, Suite #1270, Santa Ana, CA 92707 TEL: (714) 431-2320 FAX: (714) 424-0750
Sales@Toraycfa.com Technical@Toraycfa.com www.torayusa.com

TECHNICAL DATA SHEET
No. CFA-015

TORAYCA®

M46J DATA SHEET

MJ type high modulus fiber with enhanced tensile and compressive strength over ***M*** series fibers. Mainly used for premium sporting goods, aerospace, and industrial applications.

FIBER PROPERTIES

		English	Metric	Test Method
Tensile Strength		611 ksi	4,210 MPa	TY-030B-01
Tensile Modulus		63.3 Msi	436 GPa	TY-030B-01
Strain		1.0 %	1.0 %	TY-030B-01
Density		0.066 lbs/in^3	1.84 g/cm^3	TY-030B-02
Filament Diameter		2.0E-04 in.	5 μm	
Yield	6K	6,679 ft/lbs	223 g/1000m	TY-030B-03
	12K	3,347 ft/lbs	445 g/1000m	TY-030B-03
Sizing Type & Amount	50A, 50B	1.0 %		TY-030B-05
	Twist	Twisted, Untwisted		

FUNCTIONAL PROPERTIES

CTE	-0.9 α·10^{-6}/°C
Specific Heat	0.17 Cal/g·°C
Thermal Conductivity	0.202 Cal/cm·s·°C
Electric Resistivity	0.9 x 10^{-3} Ω·cm
Chemical Composition: Carbon	>99 %
Na + K	<50 ppm

COMPOSITE PROPERTIES*

Tensile Strength	320 ksi	2,210 MPa	ASTM D-3039
Tensile Modulus	38.5 Msi	265 GPa	ASTM D-3039
Tensile Strain	0.8 %	0.8 %	ASTM D-3039
Compressive Strength	155 ksi	1,080 MPa	ASTM D-695
Flexural Strength	210 ksi	1,420 MPa	ASTM D-790
Flexural Modulus	32.0 Msi	220 GPa	ASTM D-790
ILSS	11.5 ksi	8 kgf/mm^2	ASTM D-2344
90° Tensile Strength	7.0 ksi	47 MPa	ASTM D-3039

* Toray 250°F Epoxy Resin. Normalized to 60% fiber volume.

TORAY CARBON FIBERS AMERICA, INC.

M46J

COMPOSITE PROPERTIES**

Tensile Strength	315 ksi	2,160 MPa	ASTM D-3039
Tensile Modulus	35.5 Msi	245 GPa	ASTM D-3039
Tensile Strain	0.8 %	0.8 %	ASTM D-3039
Compressive Strength	145 ksi	980 MPa	ASTM D-695
Compressive Modulus	33.0 Msi	225 GPa	ASTM D-695
In-Plane Shear Strength	8.5 ksi	59 MPa	ASTM D-3518
ILSS	12.0 ksi	8.5 kgf/mm^2	ASTM D-2344
90° Tensile Strength	6.5 ksi	45 MPa	ASTM D-3039

** Toray Semi-Toughened 350°F Epoxy Resin. Normalized to 60% fiber volume.

See Section 4 for Safety & Handling information. The above properties do not constitute any warranty or guarantee of values. These values are for material selection purposes only. For applications requiring guaranteed values, contact our sales and technical team to establish a material specification document.

PACKAGING

The table below summarizes the tow sizes, twists, sizing types, and packaging available for standard material. Other bobbin sizes may be available on a limited basis.

Tow Sizes	Twist[1]	Sizing	Bobbin Net Weight (kg)	Bobbin Type[2]	Bobbin Size (mm) a	b	c	d	e	Spools per Case	Case Net Weight (kg)
6K	A	50A	1.0	II	76	82	192	126	156	16	16
	B	50B	1.0	II	76	82	192	126	156	16	16
12K	B	50B	2.0	II	76	82	192	157	156	12	24

[1] **Twist** A: Twisted yarn B: Untwisted yarn made from a twisted yarn through an untwisting process C: Never twisted yarn

[2] **Bobbin Type** See Diagram below

TYPE I

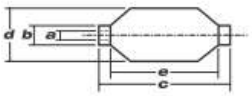

TYPE II

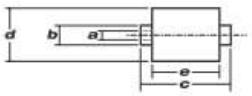

TYPE III

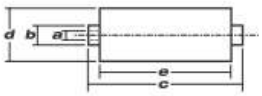

TORAY CARBON FIBERS AMERICA, INC.
6 Hutton Centre Drive, Suite #1270, Santa Ana, CA 92707 TEL: (714) 431-2320 FAX: (714) 424-0750
Sales@Toraycfa.com Technical@Toraycfa.com www.torayusa.com

TECHNICAL DATA SHEET
No. CFA-008

TORAYCA®
T1000G DATA SHEET

Intermediate modulus, world's highest tensile strength fiber. Suitable for lightweight, tensile strength critical applications such as pressure vessels for aerospace.

FIBER PROPERTIES

		English	Metric	Test Method
Tensile Strength		924 ksi	6,370 MPa	TY-030B-01
Tensile Modulus		42.7 Msi	294 GPa	TY-030B-01
Strain		2.2 %	2.2 %	TY-030B-01
Density		0.065 lbs/in^3	1.80 g/cm^3	TY-030B-02
Filament Diameter		2.0E-04 in.	5 μm	
Yield	12K	3,071 ft/lbs	485 g/1000m	TY-030B-03
Sizing Type & Amount	40D	0.7 %		TY-030B-05
	Twist	Untwisted		

FUNCTIONAL PROPERTIES

CTE	-0.55 α·10^{-6}/°C
Specific Heat	0.18 Cal/g·°C
Thermal Conductivity	0.0765 Cal/cm·s·°C
Electric Resistivity	1.4 x 10^{-3} Ω·cm
Chemical Composition: Carbon	95 %
Na + K	<50 ppm

COMPOSITE PROPERTIES*

Tensile Strength	440 ksi	3,040 MPa	ASTM D-3039
Tensile Modulus	24.0 Msi	165 GPa	ASTM D-3039
Tensile Strain	1.7 %	1.7 %	ASTM D-3039
Compressive Strength	230 ksi	1,570 MPa	ASTM D-695
Flexural Strength	230 ksi	1,570 MPa	ASTM D-790
Flexural Modulus	21.5 Msi	145 GPa	ASTM D-790
ILSS	13.0 ksi	9 kgf/mm^2	ASTM D-2344
90° Tensile Strength	8.5 ksi	60 MPa	ASTM D-3039

* Toray 250°F Epoxy Resin. Normalized to 60% fiber volume.

See Section 4 for Safety & Handling information. The above properties do not constitute any warranty or guarantee of values. These values are for material selection purposes only. For applications requiring guaranteed values, contact our sales and technical team to establish a material specification document.

TORAY CARBON FIBERS AMERICA, INC.

T1000G

PACKAGING

The table below summarizes the tow sizes, twists, sizing types, and packaging available for standard material. Other bobbin sizes may be available on a limited basis.

Tow Sizes	Twist[1]	Sizing	Bobbin Net Weight (kg)	Bobbin Type[2]	Bobbin Size (mm) a	b	c	d	e	Spools per Case	Case Net Weight (kg)
12K	B	40D	2.0	III	76.5	82.5	280	140	252	12	24

[1] **Twist** A: Twisted yarn B: Untwisted yarn made from a twisted yarn through an untwisting process C: Never twisted yarn
[2] **Bobbin Type** See Diagram below

TYPE I

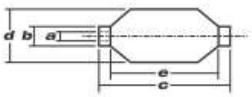

TYPE II

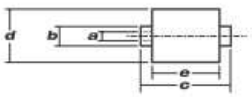

TYPE III

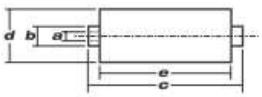

TORAY CARBON FIBERS AMERICA, INC.
6 Hutton Centre Drive, Suite #1270, Santa Ana, CA 92707 TEL: (714) 431-2320 FAX: (714) 424-0750
Sales@Toraycfa.com Technical@Toraycfa.com www.torayusa.com

LIST OF REFERENCES

[1] A. Dieitrch, "Characterization and Design of a Representative Attitude Determination and Control System of a Modern Low Earth Orbit Satellite," University of Florida, Gainesville, 2012.

[2] Union of Concerned Scientists, "UCS Satellite Database," 2012. [Online]. Available: http://www.ucsusa.org/.

[3] S. Clark, K. Lane, T. Strickland, N. Fitz-Coy and J.-C. Liou, "Defining a Typical Low Earth Orbit Satellite – Using Historical Mission Data to Aid Orbital Debris Mitigation," in *AIAA Region 2 Student Conference*, Orlando, 2012.

[4] S. Clark, A. Dietrich, M. Werremeyer, N. Fitz-Coy and J.-C. Liou, "Analysis of Representative Low Earth Orbit Satellite Data to Improve Existing Debris Models," in *AIAA Region 2 Student Conference*, Orlando, 2012.

[5] Toray Carbon Fibers America, Inc., "M55J Data Sheet," 2012. [Online]. Available: http://www.toraycfa.com/pdfs/M55JDataSheet.pdf. [Accessed 28 February 2013].

[6] Toray Carbon Fibers America, Inc., "M46J Data Sheet," 2012. [Online]. Available: http://www.cyclinside.com/upload/Category_3/Sector_21/Holder_64/Content_3002/M46JDataSheet.pdf. [Accessed 28 February 2013].

[7] Sinclair Interplanetary, "Reaction Wheels," 12 May 2012. [Online]. Available: http://www.sinclairinterplanetary.com/reactionwheels. [Accessed 13 May 2012].

[8] Sinclair Interplanetary, "Digital Sun Sensors," 12 May 2012. [Online]. Available: http://www.sinclairinterplanetary.com/digitalsunsensors. [Accessed 13 May 2012].

[9] Sinclair Interplanetary, "Torquers," 12 May 2012. [Online]. Available: http://www.sinclairinterplanetary.com/torquers. [Accessed 13 May 2012].

[10] Surrey Satellite Technology LTD, "Magnetometer," 19 July 2011. [Online]. Available: http://www.sstl.co.uk/Downloads/Datasheets/Subsys-datasheets/Magnetometer-ST0123582-v1-19-. [Accessed 13 May 2012].

[11] Surrey Satellite Technology LTD, "Altair HB+ Star Tracker (Single Unit)," 13 May 2012. [Online]. Available: http://www.sst-us.com/shop/satellite-subsystems/aocs/altair-hb--star-tracker--single-unit-. [Accessed 13 May 2012].

[12] Micro Aerospace Solutions, "Micro Aerospace Solutions," 2012. [Online]. Available: http://www.micro-a.net/imu.php. [Accessed 2 August 2012].

[13] Surrey Satellite Technology, LTD, "Microsatellite Gas Propulsion System," 25 July 2011. [Online]. Available: http://www.sstl.co.uk/Downloads/Datasheets/Subsys-datasheets/Gas-Propulsion-System-ST0065932-v004-00. [Accessed 14 February 2012].

[14] Zex, "4-6 Cylinder EFI Wet Nitrous System," 2011. [Online]. Available: http://www.zex.com/zx/4-6-cylinder-efi-wet-nitrous-system.html. [Accessed 11 April 2012].

[15] HyPerComp Engineering Inc., "Product Examples," 2012. [Online]. Available: http://www.hypercompeng.com/products.html. [Accessed 9 February 2013].

[16] Moog, "High Pressure Fill & Drain Valve," 2012. [Online]. Available: http://www.moog.com/products/propulsion-controls/spacecraft/components/fill-drain-valves/high-pressure-fill-drain-valve/. [Accessed 12 December 2012].

[17] McMaster-Carr, "Low-Profile Type 316 Stainless Steel Ball Valves," 2012. [Online]. Available: http://www.mcmaster.com/#45395K101. [Accessed 17 December 2012].

[18] The Aerospace Corporation, Spacecraft Thermal Control Handbook, vol. I: Fundamental Technologies, American Institute of Aeronautics and Astronautics, 2002.

[19] Orbital Sciences Corporation, "Minotaur IV User's Guide," January 2006. [Online]. Available: http://www.orbital.com/NewsInfo/Publications/Minotaur_IV_Guide.pdf. [Accessed 9 February 2013].

[20] Toray Industries, Inc., "Functional and Compressive Properties," 2005. [Online]. Available: http://www.torayca.com/en/techref/fcp02.html. [Accessed 10 February 2013].

BIOGRAPHICAL SKETCH

Mark Werremeyer is a Master of Science candidate at the University of Florida with a focus in Dynamics, Systems and Control. He also completed his undergraduate studies at the University of Florida and received Bachelor of Science degrees in Mechanical and Aerospace Engineering where he took various engineering and leadership roles within the Small Satellite Design Club. As a graduate student, he has performed research within the Space Systems Group lab under the direction of Dr. Norman Fitz-Coy. In this role, he was one of the primary designers and researchers behind the development of DebriSat.